

---

# Memory Inception: Latent-Space KV Cache Manipulation for Steering LLMs

---

**Andy Zeyi Liu\***  
Yale University

**Michael Zhang**  
Princeton University

**Ilana Greenberg**  
Yale University

**Adam Alnasser**  
Jump Trading

**Lucas Baker**  
Jump Trading

**John Sous\***  
Yale University

## Abstract

Steering large language models (LLMs) is usually done by either instruction prompting or activation steering. Prompting often gives strong control, but caches guidance tokens at every layer and can clutter long interactions; activation steering is compact but typically weaker and does not support large structured reminders. We introduce *memory inception* (MI), a training-free method that steers in latent attention space by inserting text-derived key-value (KV) banks only at selected layers. Rather than materializing reminder content throughout the prompt cache, MI treats steering as selective KV allocation, injecting latent slots only where the model routes to them. On matched personality-steering tasks, MI gives the best overall control-drift trade-off, remaining competitive with prompting while consistently outperforming CAA. On updateable guidance, MI supports mid-conversation behavior shifts without rewriting the visible transcript, achieving the highest post-shift alignment on Qwen3. On structured reasoning, MI outperforms visible prompting on HARDMath and PHYSICS (10/12 subject  $\times$  mode cells), serving as proxies for structured reasoning in verifiable domains, while cutting content-matched KV storage by up to 118 $\times$ . These results position MI as a powerful steering method when guidance is persistent, structured, or expensive to keep in the visible transcript.

## 1 Introduction

Language models often need *persistent guidance* rather than one-shot instructions. A user may want an assistant to maintain a personality trait across a questionnaire, preserve a tone across a multi-turn dialogue, keep a long-context fact active while answering later questions, or apply a compact checklist of reasoning heuristics to a domain benchmark. The standard solution is prompting, where reminder tokens are inserted into visible context and cached at every layer. A second family, activation steering, changes hidden states directly through learned or contrastive residual directions. These two interfaces make opposite trade-offs: prompting exposes the reminder text and stores it everywhere, while activation steering is compact but not naturally text-faithful or easily updateable.

We study a third interface: *latent attention state*. We introduce *memory inception* (MI), illustrated in Figure 1, a training-free method that encodes a descriptor, summary, retrieved fact, or task heuristic into a bank of latent key-value slots, and lets only selected attention layers/heads attend over those slots alongside the ordinary prompt tokens. The reminder

---

\*Correspondence to: [andy.liu@yale.edu](mailto:andy.liu@yale.edu) and [john.sous@yale.edu](mailto:john.sous@yale.edu).

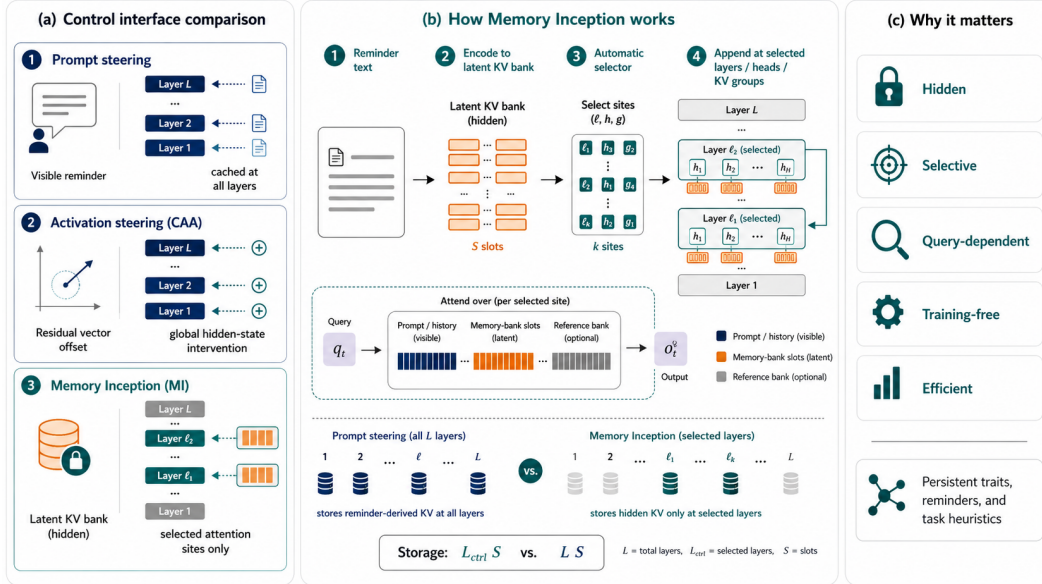


Figure 1: **Memory inception (MI)**. Concise and compact reminder text is encoded into latent KV memory-bank slots and appended only at automatically chosen layers, heads, or KV groups during decoding. Unlike prompt steering, the reminder stays outside the visible transcript at inference time and need not be stored at every layer; unlike CAA-style activation steering, the intervention acts through query-dependent attention over latent reminder slots rather than a global residual-vector offset.

is therefore available where attention reads it, rather than being repeatedly materialized as visible text or injected as a query-independent residual offset. Prompt steering stores guidance-derived KV states at every layer, even when only a small subset of layers drives control; MI instead treats guidance as a selective KV-allocation problem: identify the layers and attention units where the reminder matters, then insert latent slots only there. The layer-wise KV footprint shrinks from all  $L$  layers to  $L_{\text{ctrl}}$  controlled layers.

Conceptually, prompting and activation steering sit at opposite ends of two design axes: visible vs. latent control content, and global vs. selective intervention. MI is in the middle ground, text-conditioned but hidden from the visible transcript, and localized to the attention sites that route to it. For implicit signals such as personality, tone, or reasoning heuristics, the question becomes not whether the reminder can be cached everywhere, but where it actually needs to live.

We evaluate MI in three regimes. First, on matched personality-steering tasks where prompting, CAA, and MI receive the same control signal, we test whether latent KV steering improves the control–drift trade-off. Second, on mid-dialogue behavior shift, we test whether guidance can stay active or be updated without rewriting the visible transcript. Third, on HARDMath [Fan et al., 2025] and PHYSICS [Feng et al., 2025], we test whether the same mechanism carries reusable reasoning-heuristic banks rather than short style descriptors.

### Contributions:

- **Steering interface.** We introduce *memory inception* or MI, a training-free method that injects text-conditioned latent KV banks only at selected layers rather than materializing reminder text throughout the full prompt cache.
- **Interpretation and implementation.** We formulate the method as bank-level attention routing over prompt, target, reference, and auxiliary memories, and we give a canonical-ROPE implementation that supports dense attention, grouped-query attention, and Qwen3-style MoE models.
- **Empirical positioning.** On personality-steering tasks, MI remains competitive with prompting while consistently outperforming CAA on control–drift trade-offs. In reasoning

domains, MI acts as a training-free alternative to fine-tuning, improving PHYSICS on average and consistently outperforming the plain model on HARDMath.

- **Operating systems value.** Memory banks are most useful when guidance is persistent or structured, enabling reduction in KV storage by a factor of 6–118×.

## 2 Related Work

We keep the main-text discussion focused on the methods most directly comparable to MI and in Appendix A we list additional related works.

**Prompting and latent prompts.** Prompting remains the default inference-time interface for steering language models, from in-context instructions to chain-of-thought scaffolds [Brown et al., 2020, Wei et al., 2022, Kojima et al., 2022]. A closely related family of methods learns continuous prefixes or soft prompts that are injected into the model without changing base weights [Li and Liang, 2021, Lester et al., 2021]. MI shares the same goal of inference-time control, but differs in two ways: it is training-free, and it constructs the steering state directly from user-provided text or task heuristics at inference time rather than from optimized prompt parameters.

**Activation, attention, and cache steering.** Activation Addition and CAA steer models by adding residual directions derived from prompt pairs or positive/negative examples [Turner et al., 2024, Rimsky et al., 2024]. Representation-engineering and function-vector work likewise shows that reusable latent directions can capture high-level behaviors or in-context functions [Zou et al., 2023, Todd et al., 2024]. More recent attention-level methods, such as AutoPASTA and Spotlight, steer by reallocating attention toward instruction tokens [Zhang et al., 2024, Venkateswaran and Contractor, 2026], and KV Cache Steering manipulates cached prompt representations to induce reasoning behavior [Belitsky et al., 2025]. MI differs from these lines by appending new text-derived KV content at selected sites, so the model can attend to reusable blocks of guidance instead of compressing them into a single residual direction or a bias over visible prompt tokens.

## 3 Memory Inception: Formalism & Implementation

**Overview.** Memory inception (MI) is a training-free steering interface that encodes reminder content into latent KV banks and attaches those banks only at a small set of selected layers and attention sites, where the model can attend to them alongside ordinary prompt tokens. Figure 1 illustrates the pipeline; the following subsections formalize the intervention, bank construction, and KV-cache budget in turn.

### 3.1 Memory Inception in Latent Attention Space

We begin with the intervention interface itself: what a selected attention site sees, where the additional banks are attached, and how routing changes when more than one memory bank is present.

**Attention.** Consider one attention site in a decoder-only transformer [Vaswani et al., 2017]. At generation step  $t$ , let the live query be  $q_t \in \mathbb{R}^{d_h}$ , where  $d_h$  is the head dimension, and let the prompt/history keys and values be  $K_{\leq t}^x = [k_1^x, \dots, k_t^x]^\top$ ,  $V_{\leq t}^x = [v_1^x, \dots, v_t^x]^\top$ . The standard attention output is

$$\text{Attn}(q_t, K_{\leq t}^x, V_{\leq t}^x) = \text{softmax}\left(\frac{q_t K_{\leq t}^{x \top}}{\sqrt{d_h}}\right) V_{\leq t}^x. \quad (1)$$

MI keeps this query-dependent attention computation, but expands the candidate context at selected sites beyond visible prompt/history tokens.

**KV Cache Memory Bank.** A memory bank is a small collection of latent KV slots. Bank  $b$  contains  $M_b$  slots,

$$\mathcal{B}^{(b)} = \{(k_m^{(b)}, v_m^{(b)})\}_{m=1}^{M_b}, \quad K^{(b)} = [k_1^{(b)}, \dots, k_{M_b}^{(b)}]^\top, \quad V^{(b)} = [v_1^{(b)}, \dots, v_{M_b}^{(b)}]^\top.$$

At a selected site, MI conceptually augments the prompt cache with these slots:

$$K_t^* = \text{concat}(K_{\leq t}^x, K^{(1)}, \dots, K^{(B)}), \quad V_t^* = \text{concat}(V_{\leq t}^x, V^{(1)}, \dots, V^{(B)}). \quad (2)$$

The resulting selected-site output is  $o_t^* = \text{Attn}(q_t, K_t^*, V_t^*)$ . This augmented-cache view is the reference formulation used throughout the paper. In implementation, the ordinary prompt cache remains intact and the reminder bank is consumed as a side bank only at selected layers and units; Appendix B.1 gives the backend-specific Qwen3 details. This implements selectivity as a key design choice, as reminder slots are exposed only at layers where the controller predicts they will be useful.

**Automated Layer and Head Selection.** This selectivity is handled by an automatic calibration-time selector. Given candidate layers  $\mathcal{L}_{\text{cand}}$  and candidate attention units  $\mathcal{U}_\ell$  within each layer, the selector first scores units by how strongly their queries align with the target bank relative to a reference bank,

$$a_{\ell,u} = \max_j \frac{q_{\ell,u}^\top k_{\ell,u,j}^+}{\sqrt{d_h}} - \max_j \frac{q_{\ell,u}^\top k_{\ell,u,j}^-}{\sqrt{d_h}}. \quad (3)$$

It then keeps the top  $k$  units per layer, aggregates those scores to rank layers, and keeps the top  $m$  layers. The output is a frozen selector artifact specifying selected layers, selected units, and layer-wise gains  $\rho_\ell$ . Intuitively, MI first decides *where* reminder access should be available, and only then modifies those sites so that their queries can route more strongly toward the memory bank. The selectable unit depends on architecture: for Meta-Llama-3.1-8B-Instruct it is an attention head, while for Qwen3-30B-A3B it is a grouped-query KV group that is expanded to its associated query heads at patch time. Appendix C gives the detailed dense-head and grouped-query/KV-group selector algorithms.

**Bank-level mixture.** When only one reminder bank is present, the selected site simply chooses between prompt/history tokens and that bank. The full bank-level mixture view is most useful when several banks provide different information. Let  $b = 0$  denote the prompt bank and  $b = 1, \dots, B$  denote memory banks. Define slot scores

$$s_{t,m}^{(b)} = \frac{\langle q_t, k_m^{(b)} \rangle}{\sqrt{d_h}}, \quad \alpha_{t,m}^{(b)} = \frac{\exp(s_{t,m}^{(b)})}{\sum_r \exp(s_{t,r}^{(b)})}, \quad o_t^{(b)} = \sum_m \alpha_{t,m}^{(b)} v_m^{(b)}.$$

Let  $\tilde{\beta}_t^{(b)} = \log\left(\sum_{m=1}^{M_b} \exp(s_{t,m}^{(b)})\right) + c_t^{(b)}$  be the evidence for bank  $b$ , where  $c_t^{(b)}$  collects any bank-level gain or prior term. Then the selected-site output can be written as

$$o_t^* = \sum_{b=0}^B \tilde{\pi}_t^{(b)} o_t^{(b)}, \quad \tilde{\pi}_t = \text{softmax}([\tilde{\beta}_t^{(0)}, \dots, \tilde{\beta}_t^{(B)}]). \quad (4)$$

We use the size-normalized evidence score

$$\beta_t^{(b)} = \tilde{\beta}_t^{(b)} - \log M_b = \log\left(\frac{1}{M_b} \sum_{m=1}^{M_b} \exp(s_{t,m}^{(b)})\right) + c_t^{(b)}, \quad (5)$$

so that a larger bank does not win routing weight merely because it contains more slots. Thus, prompt, target, reference, and auxiliary banks compete through query-dependent bank evidence rather than through a global residual offset. Section 3.2 instantiates these bank-level terms for text-derived target, reference, and auxiliary memories.

### 3.2 Constructing Memory Banks

Section 3.1 treated memory banks as abstract latent objects. We now describe how reminder text is converted into reusable KV slots.

**Text-Derived Memory Banks.** Banks can be built from persona descriptors, dialogue summaries, retrieved facts, safety notes, or task heuristics. We use a shared recipe for all text-derived banks. First, the source text is placed inside one or more templates, such as a direct descriptor, an internal-principles wrapper, or a hidden-steering-note wrapper. Second, we run the wrapped text through the frozen base model and record hidden states at each token position. Third, we keep only the positions aligned to the descriptor content, unless an experiment explicitly keeps the full wrapped text. Finally, for each selected layer  $\ell$  and selected key-value unit  $u$ , the kept hidden states are normalized and projected through the model’s own key and value projections:

$$k_{\ell,u,m}^{(b)} = W_{K,u}^{(\ell)} \text{Norm}_{\ell}(h_{\ell,m}^{(b)}), \quad v_{\ell,u,m}^{(b)} = W_{V,u}^{(\ell)} \text{Norm}_{\ell}(h_{\ell,m}^{(b)}). \quad (6)$$

In our current implementation, each bank concatenates token-level slots from the original descriptor with slots from contextualized variants of the same descriptor.

**Canonical Pre-ROPE Key Storage.** Llama-style and Qwen3-style decoders use rotary position embeddings [Su et al., 2021, Grattafiori et al., 2024]. Let  $R_t$  be the rotary operator at query position  $t$ , so that  $q_t = R_t \bar{q}_t$  and prompt keys have the form  $k_j^x = R_j \bar{k}_j^x$ . A memory key stored with an arbitrary absolute rotation would be tied to the position at which the bank was constructed. We avoid this by storing memory keys in canonical pre-ROPE coordinates. For a canonical key  $\tilde{k}_m$  and optional relative phase  $\delta_m$ , the memory score is

$$s_{t,m}^{\text{mem}} = \frac{\langle R_t^{-1} q_t, R_{\delta_m} \tilde{k}_m \rangle}{\sqrt{d_h}} = \frac{\langle \bar{q}_t, R_{\delta_m} \tilde{k}_m \rangle}{\sqrt{d_h}}. \quad (7)$$

The default setting is  $\delta_m = 0$ , making the bank position-independent. For grouped-query attention, banks are stored per KV head and expanded to the query heads that share that KV group.

**Target, Reference, and Auxiliary Banks.** Many steering tasks benefit from multiple banks with different roles. We use target banks for desired behavior, optional reference banks for opposite or undesirable behavior, and auxiliary banks for additional facts or heuristics. In the contrastive setting, we first measure the target-reference evidence gap

$$\Delta_t = \log \left( \frac{1}{M^+} \sum_m e^{s_{t,m}^+} \right) - \log \left( \frac{1}{M^-} \sum_n e^{s_{t,n}^-} \right). \quad (8)$$

We then convert that gap into bank-level gains through query-adaptive gates  $g_t^{\pm} = \sigma(\pm\gamma\Delta_t)$  and define

$$\beta_t^x = \log \left( \frac{1}{T_t} \sum_j e^{s_{t,j}^x} \right), \quad (9)$$

$$\beta_t^+ = \log \left( \frac{1}{M^+} \sum_m e^{s_{t,m}^+} \right) + \rho_{\ell} \lambda_+ g_t^+, \quad \beta_t^- = \log \left( \frac{1}{M^-} \sum_n e^{s_{t,n}^-} \right) - \rho_{\ell} \lambda_- g_t^-.$$

Here  $\rho_{\ell}$  is the layer-wise gain from the selector, while  $\lambda_+$  and  $\lambda_-$  are the positive and negative bank gains. Auxiliary banks use the same bank-evidence interface with their own nonnegative gains. Bank-specific bias enters through the bank evidence terms in Eq. (9), so we do not require a separate free-form logit-bias term in the main formulation.

### 3.3 KV Cache

With bank construction and placement fixed, the main systems difference between MI and visible prompting is how much guidance-derived state must be carried across layers. For visible prompt guidance with  $T_{\text{prompt}}$  tokens in an  $L$ -layer decoder, the guidance contributes proportional KV-cache storage  $LT_{\text{prompt}}$ . A memory bank with  $S_{\text{bank}}$  slots inserted at only  $L_{\text{ctrl}}$  controlled layers contributes proportional storage  $L_{\text{ctrl}}S_{\text{bank}}$ . The idealized storage ratio is therefore

$$\text{KV ratio} = \frac{LT_{\text{prompt}}}{L_{\text{ctrl}}S_{\text{bank}}}. \quad (10)$$

For Qwen3-30B-A3B with  $L = 48$  and  $L_{\text{ctrl}} = 5$ , the equal-token/slot case gives  $48/5 = 9.6$ . If target, reference, template variants, or auxiliary banks create more latent slots than the prompt baseline uses visible tokens, Eq. (10) should be reported with the actual slot count. This accounting is why MI is most useful when guidance is persistent or structured: the reminder no longer needs to occupy the full prompt cache at every layer, even though it remains available to the selected sites that use it.

## 4 Experimental Design

**Models and Baselines.** We evaluate Meta-Llama-3.1-8B-Instruct [Meta, 2024] and Qwen3-30B-A3B Qwen Team [2025]. Across tasks, we use a consistent comparison set, consisting of the plain model, a prompt baseline that places the same guidance in visible context, CAA-style activation steering, and MI. The only model-specific difference is whether the selector chooses dense attention heads or grouped-query KV groups. For Qwen3, selector artifacts may therefore specify layer-specific KV groups rather than a single global head set. For high-throughput Qwen3 evaluation, we use vLLM [Kwon et al., 2023] for batched deterministic generation. Plain and prompt baselines run through the standard vLLM path, while intervention runs load method-specific artifacts. Appendix B.1 describes how memory-bank steering is implemented as a selected-layer side-bank attention path rather than a direct mutation of the native paged KV cache.

**Tasks and metrics.** The main evaluation covers four main settings.

- **Big Five self-evaluation.** Uses public-domain IPIP-50-style items [Goldberg et al., 2006]; the steered model answers each item with a single Likert digit. We report target shift  $\Delta_{\text{target}}$  relative to the plain model and mean absolute non-target drift  $D_{\text{non-target}}$ , summarized by the *drift-adjusted score*  $\text{DAS} = \Delta_{\text{target}} - D_{\text{non-target}}$ .
- **Big Five generation.** Steers the same traits in open-ended text; GPT-4o-mini judges target/non-target-trait presence and coherence. The main score is the *generation-adjusted score*  $\text{GAS} = \Delta_{\text{target}} - D_{\text{non-target}}$ , where  $\Delta_{\text{target}}$  is the target-score shift relative to the plain model; contrastive margin and coherence are auxiliary diagnostics (Appendix F.2).
- **Dialogue shift.** Tests whether the controller can update behavior mid-conversation under a fixed visible-context budget. The benchmark contains 204 branching cases (34 scenario roots  $\times$  {8, 16, 24} turns  $\times$  2 branches) spanning support, operational, skill-building, and planning scenarios. We report post-shift alignment  $s_{\text{target}} - s_{\text{old}}$  and judged quality; full construction details are in Appendix D.
- **HARDMath and PHYSICS.** We use these two benchmarks as proxies for structured reasoning in verifiable domains, covering applied mathematics [Fan et al., 2025] and university-level physics [Feng et al., 2025]. Task heuristics are attached as memory banks; we report normalized benchmark scores under the task-specific grading pipelines (Appendices D.4 and D.5).

**Memory-bank construction by task.** Each benchmark family uses a specific bank-construction recipe before held-out evaluation. For Big Five tasks, the bank is a target-trait descriptor with an optional opposite-trait reference; questionnaire items and generation prompts are excluded. For dialogue tasks, the bank encodes the requested target style with an optional old-style reference; future turns remain unseen. For PHYSICS and HARDMath, we prompt GPT-5.5-thinking to distill reasoning heuristics from 5 construction examples per subject or category, then strip all problem text, answers, equations, and numerical constants, leaving only natural-language process guidance. Construction examples are excluded from the evaluation set in both cases, so the bank acts as a process prior rather than retrieval over test answers. Appendix E gives representative examples.

## 5 Main Results

Table 1 and Figure 2 summarize our empirical results. MI delivers its strongest results where guidance is persistent, structured, or budget-constrained — winning decisively on PHYSICS, achieving the highest post-shift alignment on Qwen3 dialogue shift, and storing the same

Table 1: **Main results.** MI is competitive with prompting, often stronger than CAA, and extends naturally to structured reasoning with the least KV memory burden. Steering rows report DAS or GAS, dialogue rows report post-shift alignment / judged quality, and reasoning rows report benchmark score or win count. Method columns are block-specific; for structured reasoning we compare against Plain and Prompt because CAA does not provide a comparable interface for long heuristic banks. Detailed breakdowns are moved to the appendix.

Task	Model	Setting	Metric	Method		
				Prompt	CAA	Ours
<b>Steering</b>						
Big Five self-eval	Llama3.1-8B	–	DAS	0.645	0.185	<b>0.775</b>
	Qwen3-30B-A3B	–	DAS	<b>0.355</b>	0.115	0.270
Big Five generation	Llama3.1-8B	–	GAS	<b>-0.524</b>	-0.874	-0.602
	Qwen3-30B-A3B	–	GAS	0.260	-0.926	<b>0.440</b>
<b>Updateable guidance</b>						
				Prompt-init	CAA	Ours
Dialogue shift	Qwen3-30B-A3B	Overall	Align. / Quality	0.438 / 8.54	0.526 / 8.44	<b>0.816</b> / 7.75
	Qwen3-30B-A3B	24 turns	Align. / Quality	0.344 / 8.54	0.497 / 8.37	<b>0.651</b> / 7.80
	Llama3.1-8B	Overall	Align. / Quality	1.178 / 7.58	<b>1.554</b> / 7.34	1.516 / 7.00
	Llama3.1-8B	24 turns	Align. / Quality	0.964 / 7.76	<b>1.380</b> / 7.43	1.344 / 7.03
<b>Structured reasoning</b>						
				Plain	Prompt	Ours
PHYSICS	Qwen3-30B-A3B	no-CoT avg.	Score (%)	67.5	69.6	<b>70.8</b>
	Qwen3-30B-A3B	CoT avg.	Score (%)	80.3	81.2	<b>82.9</b>
	Qwen3-30B-A3B	Overall avg.	Score (%)	73.9	75.4	<b>76.9</b>
	Qwen3-30B-A3B	Win count (12 cells)	Win count	1	1	<b>10</b>
HARDMath	Qwen3-30B-A3B	CoT overall	Score (%)	60.8	<b>67.3</b>	63.8

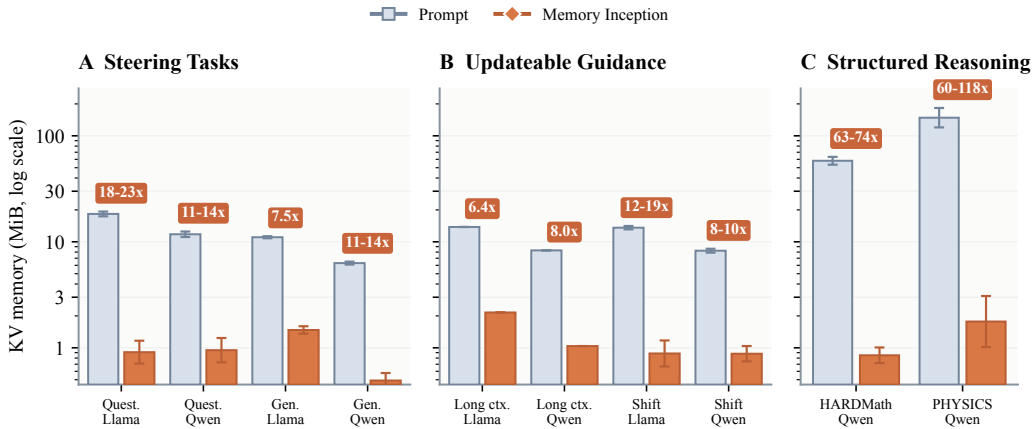


Figure 2: **KV-cache footprint of steering content.** Gray bars show the visible prompt actually used; orange bars show the budget-equivalent latent footprint of MI inferred from the full content-matched accounting. Savings badges report the corresponding content-to-bank compression ratio. The y-axis is log-scaled KV memory in MiB.

steering content at a fraction of the KV cost of visible prompting. Prompting retains an edge only in short raw-control settings where exact reminder wording can be cheaply placed in visible context.

**Competitive Steering and Updateable Guidance.** Personality steering offers the most direct comparison: all three methods receive the same control signal and differ only in where it is injected. MI stays competitive with prompting while consistently outperforming CAA, achieving the strongest DAS on Llama self-evaluation, more than doubling CAA on Qwen3 (0.270 vs. 0.115), and improving over CAA on both backbones in generation while remaining close to prompting; MI is most favorable when raw target movement would otherwise induce large collateral drift (Appendices F.1 and F.2). This advantage sharpens once the visible prompt budget is fixed after initialization: on Qwen3 dialogue shift, post-shift alignment rises from 0.438 (prompt-init) and 0.526 (CAA) to 0.816 overall, and from 0.344 to 0.651 at 24 turns. On Llama, CAA leads on raw alignment but MI remains close (1.516 vs. 1.554

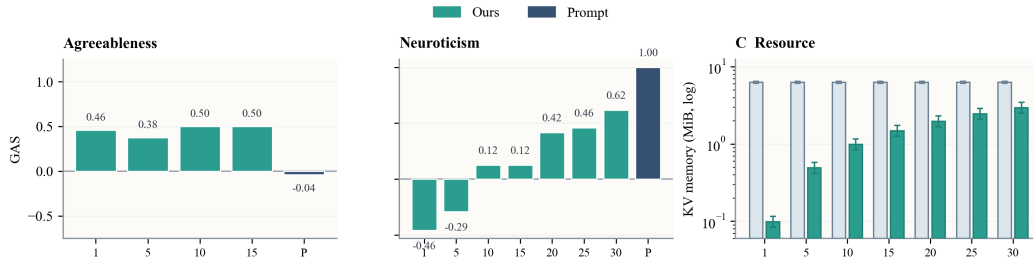


Figure 3: **Qwen3 layer-selection ablation.** Panels A and B report GAS for an easier trait (agreeableness) and a harder trait (neuroticism) as the number of selected layers increases. Panel C shows the corresponding budget-equivalent KV footprint relative to prompting.

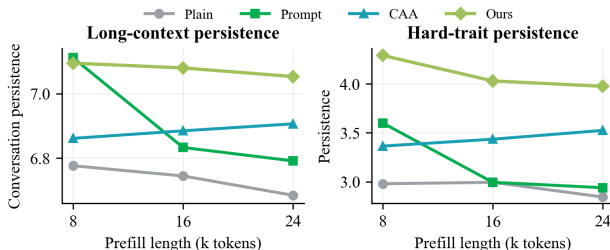


Figure 4: **Qwen3 long-context persistence under opposite-style prefills.** Left: average persistence across all six target traits. Right: the harder *dismissive+anxious* average. The full Qwen3 trait×prefill breakdown is in Appendix Table 12, and the corresponding Llama breakdown is in Appendix Table 13.

overall; 1.344 vs. 1.380 at 24 turns), marking a clear Qwen3 win for latent memory updates and a tighter Llama controllability–quality trade-off.

**Structured Reasoning from Block Guidance.** Structured reasoning is where MI’s interface matters most. A subject heuristic, global planner, and completion checklist form a reusable block of guidance natural to inject as visible text or as a latent bank, but not as a single residual direction; the reasoning rows of Table 1 therefore compare Plain, Prompt, and MI. On PHYSICS, MI is the clearest positive case: it wins 10 of the 12 subject×mode cells and the best overall average (76.9% vs. 75.4% for prompting, 73.9% for plain). HARDMath is more mixed: visible prompting leads overall at 67.3%, but MI still improves over plain (63.8% vs. 60.8%) and wins or ties plain in seven of the eight categories (Table 18). Together, these results show MI can carry reusable blocks of reasoning guidance, while prompt-faithful benchmarks can still favor visible prompting when exact heuristic wording matters.

**KV-Cache Savings.** Figure 2 reports the systems result that motivates MI beyond steering quality. MI reduces the KV footprint by 6.4× in the long-context Llama case, 60–118× on PHYSICS, and 63–74× on HARDMath. The gain grows with guidance length: short persona descriptors benefit primarily from selected-layer placement, while long heuristic banks benefit from both selected-layer placement and prompt-to-slot compression. We report KV-equivalent storage rather than allocator-level memory traces, but the trend supports MI’s central systems argument: as steering content grows longer and more reusable, latent storage becomes substantially cheaper than repeatedly materializing it in visible prompt space.

## 6 Analysis and Ablations

**Setup and scope.** In this section we present two ablation analyses on Qwen3-30B-A3B. The first is a **layer-selection ablation** (Figure 3): varying the number of selected layers

while holding bank content fixed, isolating how much latent coverage MI needs for traits of different difficulty. The second is a **long-context persistence study** (Figure 4): prepending a long opposite-style prefill before the visible interaction, testing how well each method’s steering signal survives competing context.

**Layer Ablation.** Figure 3 varies the number of selected layers while holding bank content fixed. We test two traits that bracket the difficulty range: *agreeableness*, which aligns with Qwen3’s instruction-tuned default disposition and requires only a small nudge, and *neuroticism*, which runs counter to it and is substantially harder to steer. Accordingly, for *agreeableness* a single layer already moves the trait upward and scores stabilize by ten layers; for *neuroticism*, fewer than ten layers leave the score negative, and meaningful control requires attaching the bank to a broader slice of the network. The resource panel (Panel C) shows that even the widest selected-layer settings remain below the prompt baseline in budget-equivalent KV footprint: MI requires broader coverage for harder traits, but never requires prompt-style per-layer residency to achieve useful control.

**Long-Context Persistence.** Figure 4 prepends a long opposite-style prefill before the visible interaction and measures how well each method’s steering signal survives. On the overall six-trait average (left panel), all methods degrade as the prefill grows, but MI decays least; on the harder *dismissive* and *anxious* traits (right panel), the separation is more pronounced: prompt performance drops sharply while MI preserves stronger target behavior throughout. The pattern follows directly from MI’s design: visible prompting must compete with the salience of the newly processed context, whereas latent banks reside at selected attention sites and are insensitive to earlier competing context. CAA is more stable than prompting but MI remains strongest on the hard-trait slice. Appendix D gives the evaluation setup, and Appendix Tables 12 and 13 give the full trait-by-prefill results.

**General Capability Check.** We also perform general capability check on GSM8K and MMLU after steering towards various persona. Appendix F.7 confirms that MI produces no meaningful capability degradation relative to the plain model, and less degradation than visible prompting across trait-benchmark pairs where drops occur.

## 7 Conclusion

We introduced memory inception (MI), a training-free method that steers LLMs by appending text-derived KV banks to selected attention layers, occupying the middle ground between visible prompting and activation steering. MI improves the control–drift trade-off over CAA while remaining competitive with prompting, supports mid-conversation behavior updates on Qwen3 without rewriting the visible transcript, and carries reusable heuristic blocks on PHYSICS and HARDMath. Across all settings, it reduces content-matched KV storage by 6–118× relative to visible prompting, making it most attractive when guidance is persistent, structured, or expensive to keep in context.

**Limitations.** Three aspects bound the current results. First, each task family uses a different judge and scoring protocol: personality tasks use LLM-scored Likert shifts while reasoning tasks use rubric-based partial credit, making cross-task comparisons indirect and precluding a single unified aggregate score. Second, bank quality is task-dependent: slots that are noisy, overspecific, or too broad may fail in new settings, and the selector requires task-specific calibration examples, so MI is not a zero-design interface. Third, results are partly backbone-dependent: Qwen3 shows the clearest persistent-guidance gains while Llama exhibits a sharper controllability–quality trade-off, and our cache analysis measures KV-storage footprint rather than realized latency or allocator-level VRAM. Finally, the same latent-steering mechanism that enables persistent hidden guidance could be misused for covert behavior shaping or hidden policy injection; we therefore view disclosure and auditability of steering artifacts as necessary safeguards for any real deployment.

**Responsible release.** Since latent steering can hide persistent behavioral guidance, we release only anonymous research code, evaluation scripts, and benchmark assets, not a

deployment-ready steering service or a curated bank of covert persuasion or hidden-policy artifacts. For any real deployment, latent steering should be disclosed to operators, steering-bank artifacts should be access-controlled and audit-logged, and sensitive banks should require human review before use. We view these constraints as minimum safeguards against covert behavior shaping and hidden policy injection.

## Acknowledgements

This research was supported in part by the Yale Office of the Provost. Experiments were carried out on the Yale Bouchet Cluster and Runpod. A. Alnasser and L. Baker were supported by Jump Trading.

## References

- Max Belitsky, Dawid J. Kopiczko, Michael Dorkenwald, M. Jehanzeb Mirza, James R. Glass, Cees G. M. Snoek, and Yuki M. Asano. KV cache steering for controlling frozen LLMs, 2025. URL <https://arxiv.org/abs/2507.08799>.
- Sebastian Borgeaud, Arthur Mensch, Jordan Hoffmann, Trevor Cai, Eliza Rutherford, Katie Millican, George B. M. van den Driessche, Jean-Baptiste Lespiau, Bogdan Damoc, Aidan Clark, Diego de Las Casas, Aurelia Guy, Jacob Menick, Roman Ring, Tom Hennigan, Saffron Huang, Loren Maggiore, Chris Jones, Albin Cassirer, Andy Brock, Michela Paganini, Geoffrey Irving, Oriol Vinyals, Simon Osindero, Karen Simonyan, Jack Rae, Erich Elsen, and Laurent Sifre. Improving language models by retrieving from trillions of tokens. In *Proceedings of the 39th International Conference on Machine Learning*, volume 162 of *Proceedings of Machine Learning Research*, pages 2206–2240. PMLR, 2022. URL <https://proceedings.mlr.press/v162/borgeaud22a.html>.
- Tom B. Brown, Benjamin Mann, Nick Ryder, Melanie Subbiah, Jared Kaplan, Prafulla Dhariwal, Arvind Neelakantan, Pranav Shyam, Girish Sastry, Amanda Askell, et al. Language models are few-shot learners. In *Advances in Neural Information Processing Systems*, volume 33, pages 1877–1901. Curran Associates, Inc., 2020. URL <https://papers.neurips.cc/paper/2020/hash/1457c0d6bfc4967418bfb8ac142f64a-Abstract.html>.
- Jingxuan Fan, Sarah Martinson, Erik Y. Wang, Kaylie Hausknecht, Jonah Brenner, Danxian Liu, Nianli Peng, Corey Wang, and Michael P. Brenner. HARDMath: A benchmark dataset for challenging problems in applied mathematics. In *International Conference on Learning Representations*, 2025. doi: 10.48550/arXiv.2410.09988. URL <https://openreview.net/forum?id=nDTvP6tBMd>.
- Kaiyue Feng, Yilun Zhao, Yixin Liu, Tianyu Yang, Chen Zhao, John Sous, and Arman Cohan. Physics: Benchmarking foundation models on university-level physics problem solving. In *Findings of the Association for Computational Linguistics: ACL 2025*, pages 11717–11743, Vienna, Austria, 2025. Association for Computational Linguistics. doi: 10.18653/v1/2025.findings-acl.610. URL <https://aclanthology.org/2025.findings-acl.610/>.
- Yuyao Ge, Shenghua Liu, Yiwei Wang, Tianyu Liu, Baolong Bi, Lingrui Mei, Jiayu Yao, Jiafeng Guo, and Xueqi Cheng. Prism- $\delta$ : Differential subspace steering for prompt highlighting in large language models, 2026. URL <https://arxiv.org/abs/2603.10705>.
- Lewis R. Goldberg, John A. Johnson, Herbert W. Eber, Robert Hogan, Michael C. Ashton, C. Robert Cloninger, and Harrison G. Gough. The international personality item pool and the future of public-domain personality measures. *Journal of Research in Personality*, 40(1):84–96, 2006. doi: 10.1016/j.jrp.2005.08.007. URL <https://doi.org/10.1016/j.jrp.2005.08.007>.
- Aaron Grattafiori, Abhimanyu Dubey, Abhinav Jauhri, Abhinav Pandey, Abhishek Kadian, Ahmad Al-Dahle, Aiesha Letman, Akhil Mathur, Alan Schelten, Alex Vaughan, et al. The Llama 3 herd of models, 2024. URL <https://arxiv.org/abs/2407.21783>.

- Urvashi Khandelwal, Omer Levy, Dan Jurafsky, Luke Zettlemoyer, and Mike Lewis. Generalization through memorization: Nearest neighbor language models. In *International Conference on Learning Representations*, 2020. URL <https://openreview.net/forum?id=Hk1BjCEKvH>.
- Takeshi Kojima, Shixiang Shane Gu, Machel Reid, Yutaka Matsuo, and Yusuke Iwasawa. Large language models are zero-shot reasoners. In *Advances in Neural Information Processing Systems*, volume 35. Curran Associates, Inc., 2022. URL <https://arxiv.org/abs/2205.11916>.
- Woosuk Kwon, Zhuohan Li, Siyuan Zhuang, Ying Sheng, Lianmin Zheng, Cody Hao Yu, Joseph E. Gonzalez, Hao Zhang, and Ion Stoica. Efficient memory management for large language model serving with PagedAttention. In *Proceedings of the 29th ACM Symposium on Operating Systems Principles*, pages 611–626. Association for Computing Machinery, 2023. doi: 10.1145/3600006.3613165. URL <https://doi.org/10.1145/3600006.3613165>.
- Bruce W. Lee, Inkit Padhi, Karthikeyan Natesan Ramamurthy, Erik Miehl, Pierre Dognin, Manish Nagireddy, and Amit Dhurandhar. Programming refusal with conditional activation steering. In *International Conference on Learning Representations*, 2025. doi: 10.48550/arXiv.2409.05907. URL <https://openreview.net/forum?id=0i47wc10sm>. Spotlight.
- Brian Lester, Rami Al-Rfou, and Noah Constant. The power of scale for parameter-efficient prompt tuning. In *Proceedings of the 2021 Conference on Empirical Methods in Natural Language Processing*, pages 3045–3059, Online and Punta Cana, Dominican Republic, 2021. Association for Computational Linguistics. doi: 10.18653/v1/2021.emnlp-main.243. URL <https://aclanthology.org/2021.emnlp-main.243/>.
- Patrick Lewis, Ethan Perez, Aleksandra Piktus, Fabio Petroni, Vladimir Karpukhin, Naman Goyal, Heinrich Küttler, Mike Lewis, Wen-tau Yih, Tim Rocktäschel, Sebastian Riedel, and Douwe Kiela. Retrieval-augmented generation for knowledge-intensive NLP tasks. In *Advances in Neural Information Processing Systems*, volume 33, pages 9459–9474. Curran Associates, Inc., 2020. URL <https://papers.nips.cc/paper/2020/hash/6b493230205f780e1bc26945df7481e5-Abstract.html>.
- Weixian Waylon Li, Yuchen Niu, Yongxin Yang, Keshuang Li, Tiejun Ma, and Shay B. Cohen. Spectral attention steering for prompt highlighting. In *The Fourteenth International Conference on Learning Representations*, 2026. doi: 10.48550/arXiv.2603.01281. URL <https://openreview.net/forum?id=XfLvGIFmAN>.
- Xiang Lisa Li and Percy Liang. Prefix-tuning: Optimizing continuous prompts for generation. In *Proceedings of the 59th Annual Meeting of the Association for Computational Linguistics and the 11th International Joint Conference on Natural Language Processing (Volume 1: Long Papers)*, pages 4582–4597, Online, 2021. Association for Computational Linguistics. doi: 10.18653/v1/2021.acl-long.353. URL <https://aclanthology.org/2021.acl-long.353/>.
- Meta. Model card for Meta Llama 3.1. Hugging Face model card, 2024. URL <https://huggingface.co/meta-llama/Llama-3.1-8B-Instruct>. Accessed: 2026-05-06.
- Qwen Team. Qwen3-30b-a3b model card. Hugging Face model card, 2025. URL <https://huggingface.co/Qwen/Qwen3-30B-A3B>. Accessed: 2026-05-06.
- Nina Rimsky, Nick Gabrieli, Julian Schulz, Meg Tong, Evan Hubinger, and Alexander Turner. Steering Llama 2 via contrastive activation addition. In *Proceedings of the 62nd Annual Meeting of the Association for Computational Linguistics (Volume 1: Long Papers)*, pages 15504–15522, Bangkok, Thailand, 2024. Association for Computational Linguistics. doi: 10.18653/v1/2024.acl-long.828. URL <https://aclanthology.org/2024.acl-long.828/>.
- Niklas Stoehr, Kevin Du, Vésteinn Snæbjarnarson, Robert West, Ryan Cotterell, and Aaron Schein. Activation scaling for steering and interpreting language models. In *Findings of*

- the Association for Computational Linguistics: EMNLP 2024*, pages 8189–8200, Miami, Florida, USA, 2024. Association for Computational Linguistics. doi: 10.18653/v1/2024.findings-emnlp.479. URL <https://aclanthology.org/2024.findings-emnlp.479/>.
- Jianlin Su, Yu Lu, Shengfeng Pan, Ahmed Murtadha, Bo Wen, and Yunfeng Liu. RoFormer: Enhanced transformer with rotary position embedding, 2021. URL <https://arxiv.org/abs/2104.09864>.
- Eric Todd, Millicent L. Li, Arnab Sen Sharma, Aaron Mueller, Byron C. Wallace, and David Bau. Function vectors in large language models. In *The Twelfth International Conference on Learning Representations*, 2024. URL <https://openreview.net/forum?id=AwyxyMwaG>.
- Alexander Matt Turner, Lisa Thiergart, Gavin Leech, David Udell, Juan J. Vazquez, Ulisse Mini, and Monte MacDiarmid. Steering language models with activation engineering, 2024. URL <https://arxiv.org/abs/2308.10248>.
- Ashish Vaswani, Noam Shazeer, Niki Parmar, Jakob Uszkoreit, Llion Jones, Aidan N. Gomez, Łukasz Kaiser, and Illia Polosukhin. Attention is all you need. In *Advances in Neural Information Processing Systems*, volume 30. Curran Associates, Inc., 2017. URL <https://papers.neurips.cc/paper/7181-attention-is-all-you-need>.
- Praveen Venkateswaran and Danish Contractor. Spotlight your instructions: Instruction-following with dynamic attention steering. In *Proceedings of the 19th Conference of the European Chapter of the Association for Computational Linguistics (Volume 1: Long Papers)*, pages 3752–3770, Rabat, Morocco, 2026. Association for Computational Linguistics. doi: 10.18653/v1/2026.eacl-long.174. URL <https://aclanthology.org/2026.eacl-long.174/>.
- Jason Wei, Xuezhi Wang, Dale Schuurmans, Maarten Bosma, Brian Ichter, Fei Xia, Ed H. Chi, Quoc V. Le, and Denny Zhou. Chain-of-thought prompting elicits reasoning in large language models. In *Advances in Neural Information Processing Systems*, volume 35. Curran Associates, Inc., 2022. URL <https://proceedings.neurips.cc/paper/2022/hash/9d5609613524ecf4f15af0f7b31abca4-Abstract-Conference.html>.
- Yuhuai Wu, Markus N. Rabe, DeLesley Hutchins, and Christian Szegedy. Memorizing transformers. In *International Conference on Learning Representations*, 2022. URL <https://openreview.net/forum?id=TrjbxzRcnf->.
- Zhengxuan Wu, Qinan Yu, Aryaman Arora, Christopher D. Manning, and Christopher Potts. Improved representation steering for language models, 2025. URL <https://arxiv.org/abs/2505.20809>.
- An Yang, Anfeng Li, Baosong Yang, Beichen Zhang, Binyuan Hui, Bo Zheng, Bowen Yu, Chang Gao, Chengen Huang, Chenxu Lv, et al. Qwen3 technical report, 2025. URL <https://arxiv.org/abs/2505.09388>.
- Qingru Zhang, Xiaodong Yu, Chandan Singh, Xiaodong Liu, Liyuan Liu, Jianfeng Gao, Tuo Zhao, Dan Roth, and Hao Cheng. Model tells itself where to attend: Faithfulness meets automatic attention steering, 2024. URL <https://arxiv.org/abs/2409.10790>.
- Andy Zou, Long Phan, Sarah Chen, James Campbell, Phillip Guo, Richard Ren, Alexander Pan, Xuwang Yin, Mantas Mazeika, Ann-Kathrin Dombrowski, Shashwat Goel, Nathaniel Li, Michael J. Byun, Zifan Wang, Alex Mallen, Steven Basart, Sanmi Koyejo, Dawn Song, Matt Fredrikson, J. Zico Kolter, and Dan Hendrycks. Representation engineering: A top-down approach to AI transparency, 2023. URL <https://arxiv.org/abs/2310.01405>.

## Appendix contents

- [Additional related work](#)
- [Models, inference stack, and hardware](#)
- [Automated attention head/layer selection](#)
- [Datasets and evaluation](#)
- [Examples of memory/heuristic banks](#)
- [Results breakdown by task](#)
- [Technical derivations](#)

### A Additional related work

Beyond the direct prompting and activation-steering baselines in the main text, MI also sits near a broader family of inference-time memory mechanisms. Retrieval-augmented generation, kNN-LMs, Memorizing Transformers, and RETRO augment the model with non-parametric external memory at inference time [Lewis et al., 2020, Khandelwal et al., 2020, Wu et al., 2022, Borgeaud et al., 2022]. Those methods primarily target factual recall or language-model quality by retrieving passages or neighbors, whereas MI uses compact text-derived banks to carry behavior or reasoning heuristics.

A second neighboring line of work studies latent steering with more selective interventions than a single residual-vector addition. Activation Scaling, Improved Representation Steering, and conditional activation steering refine how steering directions are normalized, composed, and conditionally activated [Stoehr et al., 2024, Wu et al., 2025, Lee et al., 2025]. These methods support the general claim that useful control can be achieved without retraining, but they still operate through residual-space interventions rather than through reusable latent KV content.

Recent attention-path methods are even closer in spirit. Spotlight dynamically increases attention to designated instructions, while SEKA and Prism- $\Delta$  steer key representations or attention subspaces to highlight visible prompt spans [Venkateswaran and Contractor, 2026, Li et al., 2026, Ge et al., 2026]. KV Cache Steering intervenes directly in the cache to induce controlled behavior in otherwise frozen models [Belitsky et al., 2025]. MI differs from these approaches in its interface: instead of reweighting visible prompt tokens alone, it stores multi-sentence target, reference, or heuristic guidance as latent side-bank slots that can be updated independently of the visible transcript.

### B Models, inference stack, and hardware

Table 2 summarizes the two backbones used in the experiments, using the public model cards and technical reports [Meta, 2024, Grattafiori et al., 2024, Qwen Team, 2025, Yang et al., 2025]. We keep the official Qwen3-30B-A3B naming: “A3B” refers to roughly 3.3B activated parameters, while the model card separately reports eight activated experts.

Table 2: **Model details.** Public model-card facts for the two experimental backbones.

Model	Size and context	Architecture notes	License
Meta-Llama-3.1-8B-Instruct	8B parameters; 128k context	Meta autoregressive Transformer; text-only multilingual instruction model; SFT/RLHF tuning; GQA; December 2023 knowledge cutoff	Llama 3.1 Community
Qwen3-30B-A3B	30.5B total and 3.3B activated parameters; 32,768 native context; 131,072 with YaRN	Qwen Team causal MoE LM; pre/post-trained; 48 layers; 32 Q heads and 4 KV heads; 128 experts and 8 activated experts	Apache 2.0

Meta-Llama-3.1-8B-Instruct is a text-only multilingual instruction-tuned assistant model with grouped-query attention and the Llama 3.1 Community License. Qwen3-30B-A3B is a sparse MoE causal language model with thinking and non-thinking generation modes, grouped-query attention with four KV heads, and an Apache 2.0 license. These architectural differences motivate the separate dense-head and grouped-query/KV-group selector treatments in Section 3.

Across experiments, we ran on whichever GPU was available on the cluster at execution time, primarily NVIDIA H100, H200, B200, or RTX Pro 6000 Blackwell GPUs. We treat the hardware fleet as execution infrastructure rather than as an experimental factor: within each evaluated sweep, backbone, bank, and comparison method are held fixed, while the exact GPU model may vary with cluster availability.

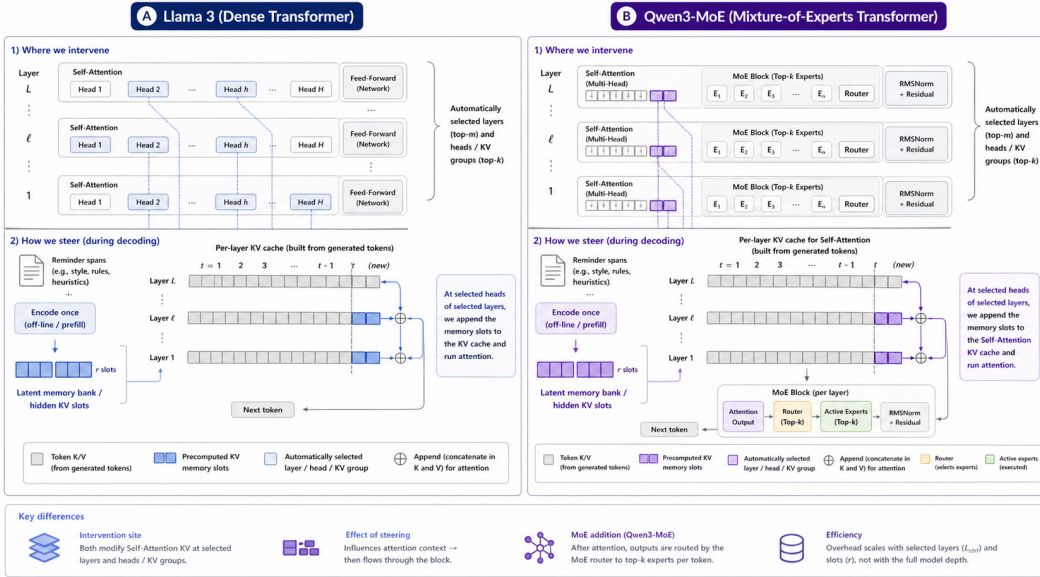


Figure 5: **Architectural placement of memory-bank attention steering.** The same intervention concept applies to both dense Llama-style decoders and Qwen3-MoE decoders: reminder spans are encoded into latent memory-bank slots, an automatic selector chooses a small set of layers and attention sites, and the selected sites attend over those slots during decoding. In dense attention the selectable unit is an attention head; in Qwen3 grouped-query attention the selectable unit can be a KV group that expands to its associated query heads before the downstream MoE block. The diagram is a conceptual cache schematic; backend-specific implementations may realize the appended memory as a selected-site side bank rather than by directly modifying the native paged KV cache.

## B.1 vLLM inference implementation

We use vLLM for high-throughput batched inference in the Qwen3 experiments. Plain and prompt baselines require no model change. Post-attention CAA is also comparatively simple: it adds a layer-specific vector after the projected attention output and before that output rejoins the residual stream.

Memory-bank steering requires a deeper attention-path integration. Although Eq. (2) describes the reference method as appending latent slots to the available keys and values, the Qwen3 vLLM implementation should not be read as directly mutating vLLM’s native paged KV cache. vLLM continues to manage the ordinary prompt and generated-token cache, while the reminder bank is represented as a side KV bank consumed only at selected layers and heads or KV groups.

At a selected Qwen3 layer, the intervention branch obtains the live query states, applies the same QK normalization and rotary-position treatment as the base model, and uses

---

**Algorithm 1** Automatic layer and head/KV-group selection

---

**Input:** candidate layers  $\mathcal{L}_{\text{cand}}$ ; candidate units  $\mathcal{U}_\ell$  for each layer; calibration prompts  $\mathcal{C}$ ; target and reference banks; budgets  $m$  layers and  $k$  units per layer; steering gains and selector scoring rule.

**Output:** a frozen selector artifact  $\mathcal{A}$  specifying selected layers, selected heads or KV groups, layer-wise gains  $\rho_\ell$ , and calibration diagnostics.

1. Construct target and reference memory banks from the wrapped reminder spans.
  2. Run the calibration prompts with diagnostic tracing enabled over the candidate layer/unit sites. Record target-reference alignment, target-bank mass, reference-bank mass, prompt-bank mass, and phrase-level bank engagement.
  3. Compute unit scores  $U_{\ell,u}$  from Eq. (11). For each layer, set  $\hat{\mathcal{U}}_\ell \leftarrow \text{TopK}_u(U_{\ell,u}, k)$ .
  4. Compute layer scores  $U_\ell$  from Eq. (12) by aggregating the top-unit scores within each layer, and set  $\hat{\mathcal{L}} \leftarrow \text{TopM}_\ell(U_\ell, m)$ .
  5. In dense attention, the selected unit  $u$  is a query head. In grouped-query attention,  $u$  is a KV group expanded to its associated query heads at patch time.
  6. Export  $\mathcal{A} = \{\hat{\mathcal{L}}, \{\hat{\mathcal{U}}_\ell\}_{\ell \in \hat{\mathcal{L}}}, \{\rho_\ell\}, \text{diagnostics}\}$  and freeze it before held-out evaluation.
- 

the pre-ROPE normalized query representation for reminder-bank scoring. The current vLLM path treats the already-computed selected-head attention output as the prompt-bank output and uses a synthetic single-slot prompt-bank score for bank-level routing. This is an approximation to Eq. (4): target and optional reference bank outputs are computed from precomputed side-bank keys and values, but the prompt side is not reconstructed from the full native paged prompt KV cache. The mixed selected-site output is written back before the attention output projection. For Qwen3 grouped-query attention, the selector artifact stores KV groups and the patch expands each selected group to the query heads that share it.

## C Automated attention head/layer selection

The selector is fit automatically on a small calibration split before held-out evaluation. In the dense Llama-style questionnaire runs reported here, the calibration pass records attention-route diagnostics rather than directly optimizing a task score at every site. The recorded statistics include target/reference alignment margins, prompt-bank mass, target-bank mass, reference-bank mass, and phrase-level bank engagement. More general selectors could replace these diagnostics with task-level target and drift objectives, but the reported results use the frozen diagnostic procedure summarized in Algorithm 1.

**Stage 1: unit ranking.** Let  $\mathcal{L}_{\text{cand}}$  be the set of candidate layers and  $\mathcal{U}_\ell$  the selectable units in layer  $\ell$ . For the diagnostic selector, each candidate site receives the score

$$U_{\ell,u} = \bar{a}_{\ell,u} + \xi \bar{m}_{\ell,u}^+ - \chi \bar{m}_{\ell,u}^x, \quad (11)$$

where  $\bar{a}_{\ell,u}$  is the average target-versus-reference alignment margin from Eq. (3),  $\bar{m}_{\ell,u}^+$  is mean target-bank mass, and  $\bar{m}_{\ell,u}^x$  is mean prompt-bank mass. In the dense questionnaire calibration, the primary ordering is by  $\bar{a}_{\ell,u}$ , with target-bank mass used as a tie-break and engagement diagnostic. We keep the top  $k$  units per layer.

**Stage 2: layer ranking.** Layer scores aggregate the selected unit scores:

$$U_\ell = \text{AggTopK}_{u \in \mathcal{U}_\ell}(U_{\ell,u}; k), \quad (12)$$

where AggTopK is either a sum or mean over the layer’s top  $k$  unit scores. We keep the top  $m$  layers by  $U_\ell$ . A task-specific selector could instead use a direct utility such as target movement minus drift movement, but that is not the frozen objective used for the questionnaire artifacts reported here.

**Selector artifact and evaluation.** The selector output is a reusable artifact containing the selected layers, selected heads or KV groups per layer, the layer gain schedule  $\rho_\ell$ , bank-mass diagnostics, target/reference alignment margins, and the calibration configuration. At inference time, no further search is performed: the model loads this artifact, constructs banks for the requested reminder, and applies attention steering only at the stored sites. All reported test results are then produced on held-out data with the same frozen selector for plain, prompt, CAA, and memory-bank comparisons.

## D Datasets and evaluation

Across all tasks, banks are frozen before held-out evaluation. When a benchmark needs construction examples to induce process cards, those construction examples are excluded from the scored pool. Representative bank content is collected later in Appendix E.

Asset and terms summary: Meta-Llama-3.1-8B-Instruct is used under the Llama 3.1 Community License, and Qwen3-30B-A3B under Apache 2.0, following their official model cards. The IPIP-50 questionnaire items are public-domain. HARDMath, PHYSICS, GSM8K, and MMLU are used from their original public benchmark releases and therefore follow those original release terms; the anonymous repository linked in the abstract points to the exact evaluation assets. GPT-4o-mini and GPT-5.5-thinking are accessed only through the OpenAI API under the provider’s service terms and are used only as evaluation judges, not redistributed as paper assets.

### D.1 Big Five self-evaluation

The questionnaire benchmark uses IPIP-50 Big Five items [Goldberg et al., 2006]. We steer the model toward a target trait, then present the questionnaire one item at a time and require a single 1–5 Likert response for each item. Reverse-keyed items are rescored before trait aggregation. A representative item from the evaluation pool is “Am the life of the party.” The target metric is the change in the steered trait relative to the plain model, and non-target drift is the mean absolute change over the other four traits.

### D.2 Big Five generation

The generation benchmark uses the same target traits but measures them on free-form responses rather than questionnaire digits. A representative held-out prompt is “Write a brief reply to a person feeling uncertain before an interview.” Responses are evaluated by an external LLM judge, GPT-4o-mini, which scores target-trait presence, opposite-trait pressure, the five Big Five traits, and coherence on a 1–5 scale. From these judgments we compute target-trait movement, non-target drift, and contrastive margins.

### D.3 Dialogue shift

We construct the dialogue benchmark as a bank of multi-turn user trajectories rather than independent single-turn prompts. The corpus contains 34 scenario roots, each instantiated at 8, 16, and 24 turns with two branches per length, for  $34 \times 3 \times 2 = 204$  cases. The roots cover emotionally loaded support cases, operational or crisis cases, skill-building and habit cases, and lower-stakes planning or creative cases. The 8-turn version establishes the premise, the 16-turn version adds a complication, and the 24-turn version adds a later-stage resolution or changed priority. The A/B branches share the same root but vary concrete details so that success requires tracking the evolving user state.

The dialogue-shift benchmark is derived from the same case bank to test whether steering can change behavior midway through an ongoing conversation. For the primary tier we use the 68 eight-turn cases; for the stress tier we use all 204 cases. Each scenario root is assigned one of six trait transitions, **warm**→**assertive**, **assertive**→**warm**, **formal**→**cautious**, **cautious**→**formal**, **dismissive**→**anxious**, or **anxious**→**dismissive**. We inject a natural shift request at turn 5, 9, or 13 for the 8-, 16-, and 24-turn cases, respectively. One representative shift turn is: “Please switch gears. Be more anxious, worried, and uncertain from here on. I got one lukewarm reply and now I feel silly again. How should I recover?”

Table 3: **Representative dialogue cases.** Examples are shortened user turns; full cases are stored as ordered turn lists.

Case	Family	Example turns
Career transition coach	Coaching/ support	<i>t1</i> : “I keep thinking about leaving my current field, but I feel embarrassed that I waited so long.” <i>t14</i> : “I spent 12 hours on the assignment and they rejected me with a generic automated email.”
Software outage crisis	Operational/ crisis	The user begins with an urgent service failure, later updates the assistant with debugging outcomes, stakeholder pressure, and recovery decisions.
Study partner dialogue	Learning/ habit	The user asks for help with a study plan, then returns with confusion, small wins, and exam-preparation constraints that must remain consistent across turns.
Friendship drift support	Relationships	<i>t1</i> : “My best friend of ten years has been dodging my calls.” <i>t24</i> : “Give me a framework for deciding how much time and energy I should invest in this renewed, but much more distant, relationship.”

For scoring, we evaluate only post-shift assistant turns with GPT-4o-mini. Let  $s_{\text{target}}$  be the score of the requested new trait and  $s_{\text{old}}$  the score of the old trait. The primary adaptation metric is  $\text{Align} = s_{\text{target}} - s_{\text{old}}$ . We also report the mean post-shift turn-quality score  $Q_{\text{turn}}$ , defined as the average of usefulness, specificity, current-turn relevance, and non-genericness. The main comparison keeps the visible prompt and KV budget fixed after initialization; prompt replacement is treated only as a higher-cache audit condition.

#### D.4 HARDMath

HARDMath [Fan et al., 2025] provides the applied-mathematics stress test. Our intended evaluation protocol is to sample 60 questions per category when available across the integral, Laplace-integral, ODE, polynomial-roots, and nondimensionalization families, then grade final boxed answers with partial credit. The current appendix tables retain the benchmark’s reported subcategory split and the scored snapshot used in this draft, but the grading protocol is the one stated here.

The original automatic scorer was too brittle for mathematically equivalent expressions, for example treating  $\frac{1}{20}$  and 0.05 as different answers. We therefore regrade with GPT-5.5-thinking plus human review. Each answer receives 0, 0.5, or 1 point. Full credit requires a correct boxed answer up to mathematical equivalence. Partial credit is assigned when the boxed answer is only partly complete but still captures a requested component of the official answer, for example when a problem asks for both lower and upper asymptotic behavior and the model gives only one asymptote.

The HARDMath banks are process-only heuristic cards distilled from held-out construction examples. Plain receives only the benchmark problem, Prompt receives the same heuristic guidance in visible context, and Ours stores the same guidance as latent memory-bank slots.

#### D.5 PHYSICS

The PHYSICS benchmark tests whether memory banks can carry reusable problem-solving heuristics rather than persona reminders. We use the text-only PHYSICS split and evaluate up to 100 questions per subject when available across classical mechanics, quantum mechanics, thermodynamics/statistical mechanics, electromagnetism, atomic physics, and optics. Subject-specific heuristic cards are distilled from held-out construction questions and then stripped of source question text, answer fragments, numerical constants, and solution-order traces before evaluation.

We grade answers with a question-specific rubric and run GPT-5.5-thinking three times per answer, reporting the average normalized score. The rubric is still partial-credit based: a score of 5 means correct, 4 means mostly correct with a minor issue, 3 means substantial partial credit, 2 means some correct setup but major errors or incompleteness, 1 means very weak progress, and 0 means wrong or unusable. We evaluate both a no-CoT setting and a CoT setting, where Qwen3 thinking mode is enabled.

## D.6 Long-context persistence

Long-context persistence uses the same 204 dialogue cases as the shift benchmark, but now the stressor is a long opposite-style prefill rather than an explicit behavior change request. Before the task dialogue begins, we prefill the visible context with non-task assistant-history text written in an opposing trait. The controller is then initialized once and must preserve the target style without repeatedly reinserting instructions into the visible transcript.

GPT-4o-mini scores every assistant turn on six style dimensions and four turn-quality dimensions, and it also scores the full conversation on target-style persistence, coherence, user-state consistency, non-repetitiveness, and overall quality. Tables 12 and 13 report  $P/T/Q$ : conversation-level target persistence, mean turn-level target style score, and conversation-level overall quality, all on 1–10 scales.

## D.7 GSM8K and MMLU

We use GSM8K and MMLU only as coarse capability checks after steering. The reported Qwen3 runs use 200 GSM8K questions and 500 MMLU questions. These benchmarks are not used to tune the steering artifacts; they serve only to confirm that persona steering does not introduce obvious capability collapse on standard reasoning and knowledge tasks.

## E Examples of memory/heuristic banks

This section consolidates representative bank content across persona, dialogue, PHYSICS, and HARDMath. The examples illustrate the kinds of process reminders stored in the latent bank, not additional scored evaluation cases.

Table 4: **Representative memory-bank construction recipes.** Banks are frozen before evaluation. Structured-reasoning construction examples are excluded from the reported test pool, and the final cards retain only general process guidance.

Task family	Source material	Example bank content	Leakage / budget control
Big Five self-evaluation and generation	Target-trait descriptor, optional opposite-trait descriptor, and wrapper variants such as direct descriptor or hidden steering note.	For an <b>assertive</b> bank: emphasize direct recommendations, explicit trade-offs, concrete next steps, and confident prioritization while avoiding avoidant or overly deferential phrasing.	No questionnaire item, generation prompt, or judged output is included in the bank text. The same frozen descriptor bank is used across held-out prompts.
Long-context persistence and dialogue shift	Target style descriptor, optional old-style/reference descriptor, and, for shift settings, the requested new style after the shift.	For a <b>dismissive</b> → <b>anxious</b> shift: target slots encode worried, uncertain, risk-sensitive language, while reference slots encode the old dismissive style so routing can suppress old-trait carryover.	Future dialogue turns are never used to build the bank. Prompt-init baselines keep a fixed visible-context budget; memory banks update latent guidance without adding repeated prompt tokens.
PHYSICS	For each subject, 5–10 construction questions and reference solutions plus standard subject knowledge. GPT-5.5-thinking distills subject-level process heuristics.	For quantum mechanics: first classify whether the problem asks for spectra, time evolution, measurement statistics, perturbative response, or asymptotics; choose a representation that simplifies the relevant operator; keep amplitudes, phases, probabilities, and observables distinct.	Construction question ids are excluded from evaluation. Final cards remove answer fragments, numeric constants, source-specific formulas, and solution-order traces.
HARDMath	For each category, 5–10 construction problems and reference solutions plus a category label. GPT-5.5-thinking distills category-level setup and checking heuristics.	For Laplace-integral problems: identify the transform parameter and convergence domain, choose differentiation under the integral, parameter substitution, or known-transform reduction, then verify by limits or differentiation before giving the final expression.	Construction problems are excluded from evaluation. Final cards describe method selection and answer checks, not solved examples or category-specific target answers.

Table 5: **Representative subject-specific heuristic cards in the PHYSICS heuristic-completion banks (part I)**. The memory-bank condition stores cards like these as latent KV slots; the prompt baseline exposes the same card text visibly. Each row is a process reminder, not a solved example.

Subject	Trigger and key idea	Action	Trap and check
Classical mechanics	A mechanics prompt mixes forces, energy, impacts, constraints, frames, and small-parameter language; mechanics errors often come from solving the wrong mode of problem.	Decide whether the task is force balance, constrained motion, impulse/collision, orbital reduction, normal-mode analysis, fluid scaling, or relativistic kinematics before writing equations.	Avoid treating every mechanics problem as Newton’s second-law integration. The selected mode should produce the requested observable with the fewest extra unknowns.
Electromagnetism	Conductors, dielectrics, magnetic media, interfaces, cavities, or coaxial geometry appear; interfaces and material response often determine unknown constants and surface sources.	Write the relevant normal and tangential boundary conditions, constitutive relations, and conductor constraints before solving the bulk field.	Avoid solving the differential equation in each region but forgetting how the regions communicate. Fields and potentials should satisfy the stated material behavior and interface jumps or continuities.
Quantum mechanics	A prompt mixes states, operators, spectra, measurement, and time language; separate spectral, dynamical, measurement, and approximation questions before computing.	Decide whether the answer concerns allowed states, time evolution, measurement statistics, response to a small change, or asymptotic behavior.	Avoid solving the wrong kind of quantum problem because similar symbols appear in the prompt. The mathematical object in the final answer should match the physical question.

Table 6: **Representative subject-specific heuristic cards in the PHYSICS heuristic-completion banks (part II).**

Subject	Trigger and key idea	Action	Trap and check
Atomic physics	Hydrogenic, helium-like, molecular, fine, hyperfine, Zeeman, Stark, or nuclear effects appear together; atomic reasoning starts from a hierarchy of scales and then adds corrections in order.	Identify the baseline structure, then place spin, relativistic, field, exchange, finite-size, or nuclear corrections by relative size.	Avoid mixing correction mechanisms without deciding which is the unperturbed problem and which is small. Each splitting or shift should be attributable to a named interaction and ordering assumption.
Optics	Lenses, mirrors, apertures, slits, gratings, coherence, or diffraction all appear possible; ray optics tracks paths and images, while wave optics tracks phase, coherence, and aperture-limited structure.	Decide whether wavelength and phase are essential or whether geometric imaging is sufficient for the requested scale.	Avoid using geometric imaging where diffraction or interference sets the answer, or adding wave machinery to a pure imaging geometry. The chosen model should depend on wavelength only when wave effects are relevant.
Thermodynamics/ statistical mechanics	Energy, volume, temperature, particle number, chemical potential, or reservoir contact is specified; the ensemble is fixed by what is controlled and what can fluctuate.	Choose microcanonical, canonical, grand-canonical, isothermal-isobaric, or another potential from the constraints before differentiating.	Avoid using a partition function whose natural variables do not match the physical setup. Later derivatives should be taken with respect to the natural variables of the chosen potential.

Table 7: **Representative HARDMath heuristic cards.** The prompt baseline exposes the same process cards as visible text, while the memory-bank condition stores them as latent slots. These cards are distilled from held-out construction examples but do not contain solved examples or answer fragments.

Category	Trigger and key idea	Action	Trap and check
Integral and Laplace-integral	The problem contains a parameterized integral, transform-like kernel, or special-function-looking expression; success often depends on choosing the right representation before manipulating the integral.	Identify the transform parameter and convergence domain, then choose among substitution, differentiation under the integral, contour/symmetry reduction, or known-transform matching.	Do not simplify outside the valid domain. Check the final expression by limits, differentiation with respect to the parameter, or a simple numeric substitution.
ODE	The prompt asks for a function satisfying differential constraints, boundary conditions, or asymptotic behavior; the equation type should be classified before solving.	Separate homogeneous and particular structure, identify singular points or conserved quantities, and use boundary data only after the general solution family is clear.	Avoid fitting constants before verifying the solution form. Substitute the final solution back into the differential equation and boundary conditions.
Polynomial roots	The prompt asks for roots, symmetric functions of roots, or parameter constraints; direct root-finding is often less stable than structural identities.	Use Vieta relations, resultants, multiplicity conditions, sign/interval arguments, or transformations that expose symmetry before expanding.	Avoid extraneous roots introduced by squaring or substitution. Check multiplicities and substitute candidate roots into the original polynomial.
Nondimensionalization	The prompt mixes physical dimensions, symbolic groups, or numeric scale choices; the target is usually an invariant dimensionless relation rather than a raw computation.	List base dimensions, form independent dimensionless groups, then decide whether the task needs symbolic simplification or numeric evaluation.	Avoid adding quantities with incompatible units or overfitting a scale choice. Verify that every reported group is dimensionless and independent.

## F Results breakdown by task

### F.1 Big Five self-evaluation

For readability, we split the detailed per-trait appendix results by backbone and give each metric its own column rather than packing four values into one cell.

Table 8: **Big Five questionnaire self-evaluation on Meta-Llama-3.1-8B-Instruct.** Columns report target-trait score, target shift from the plain model, non-target drift, and drift-adjusted score, where  $DAS = \Delta_{\text{target}} - D_{\text{non-target}}$ . Bold indicates the highest DAS among steering methods within each trait.

Trait	Method	Score	Shift	Drift	DAS
Openness	Plain	3.5	0.0	0.000	0.000
	Prompt	4.1	+0.6	0.350	0.250
	CAA	3.8	+0.3	0.050	0.250
	Ours	4.6	+1.1	0.175	<b>0.925</b>
Conscientiousness	Plain	3.9	0.0	0.000	0.000
	Prompt	4.2	+0.3	0.625	-0.325
	CAA	4.3	+0.4	0.025	0.375
	Ours	4.9	+1.1	0.100	<b>1.000</b>
Extraversion	Plain	2.8	0.0	0.000	0.000
	Prompt	4.7	+1.9	0.350	<b>1.550</b>
	CAA	2.9	+0.1	0.225	-0.125
	Ours	3.0	+0.2	0.050	0.150
Agreeableness	Plain	4.7	0.0	0.000	0.000
	Prompt	4.9	+0.2	0.250	-0.050
	CAA	4.7	+0.0	0.075	-0.075
	Ours	4.9	+0.2	0.125	<b>0.075</b>
Neuroticism	Plain	2.0	0.0	0.000	0.000
	Prompt	4.5	+2.5	0.700	<b>1.800</b>
	CAA	2.7	+0.7	0.200	0.500
	Ours	4.3	+2.3	0.575	1.725
Average	Plain	-	0.0	0.000	0.000
	Prompt	-	+1.10	0.455	0.645
	CAA	-	+0.30	0.115	0.185
	Ours	-	+0.98	0.205	<b>0.775</b>

The per-trait tables clarify that the aggregate Pareto picture in Table 1 is not uniform across all traits. Prompting remains strongest for the largest raw movement on extraversion and neuroticism, while memory-bank steering is strongest on several drift-adjusted rows, especially openness and agreeableness on Qwen3 and openness, conscientiousness, and agreeableness on Llama.

### F.2 Big Five generation

For readability, we again separate the detailed results by backbone and give each reported quantity its own column.

The generation tables show why the main-text claim is improvement over CAA rather than universal dominance over prompting. Memory-bank steering improves over CAA on the average Llama and Qwen3 generation metrics, but prompt remains the strongest visible-context baseline on several drift-adjusted rows, especially on Qwen3.

### F.3 Long-context persistence

Qwen3 shows the clearest positive long-context cases under the budget-matched setup, especially on the more difficult low-baseline traits. Llama behaves differently: prompt remains the strongest raw persistence mechanism on average, while the latent methods trade off persistence against judged quality more sharply.

Table 9: **Big Five questionnaire self-evaluation on Qwen3-30B-A3B**. Columns report target-trait score, target shift from the plain model, non-target drift, and drift-adjusted score, where  $DAS = \Delta_{\text{target}} - D_{\text{non-target}}$ . Bold indicates the highest DAS among steering methods within each trait.

Trait	Method	Score	Shift	Drift	DAS
Openness	Plain	4.1	0.0	0.000	0.000
	Prompt	4.8	+0.7	0.475	0.225
	CAA	4.4	+0.1	0.075	0.025
	Ours	4.6	+0.5	0.100	<b>0.400</b>
Conscientiousness	Plain	4.5	0.0	0.000	0.000
	Prompt	4.9	+0.4	0.525	-0.125
	CAA	4.5	+0.1	0.075	<b>0.025</b>
	Ours	4.6	+0.1	0.150	-0.050
Extraversion	Plain	3.6	0.0	0.000	0.000
	Prompt	5.0	+1.4	0.500	<b>0.900</b>
	CAA	3.7	+0.1	0.100	0.000
	Ours	3.8	+0.2	0.150	0.050
Agreeableness	Plain	4.2	0.0	0.000	0.000
	Prompt	5.0	+0.8	0.500	0.300
	CAA	4.3	+0.3	0.075	0.225
	Ours	4.9	+0.7	0.150	<b>0.550</b>
Neuroticism	Plain	2.5	0.0	0.000	0.000
	Prompt	3.6	+1.1	0.625	<b>0.475</b>
	CAA	2.8	+0.4	0.100	0.300
	Ours	3.0	+0.5	0.100	0.400
Average	Plain	-	0.0	0.000	0.000
	Prompt	-	+0.88	0.525	<b>0.355</b>
	CAA	-	+0.20	0.085	0.115
	Ours	-	+0.40	0.130	0.270

#### F.4 Dialogue shift

For readability, the appendix tables below foreground the two primary post-shift outcomes: adaptation alignment  $\text{Align} = s_{\text{target}} - s_{\text{old}}$  and judged turn quality  $Q_{\text{turn}}$ . The raw target-style and old-style component scores are omitted from the paper-level tables and remain available in the released results.

The shift tables show the main matched-budget pattern from the paper: Qwen3 provides the clearest positive cases for latent behavior updates, especially on difficult transitions such as `dismissive`→`anxious`, while Llama shows a sharper quality trade-off even when alignment improves.

#### F.5 PHYSICS results

The PHYSICS results support the structured-heuristic use case: memory banks are most helpful when the benchmark rewards reusable subject-level process reminders rather than persona changes. Gains are especially visible in CoT mode, where the latent heuristic cards can guide longer reasoning traces without occupying visible prompt budget.

#### F.6 HARDMath results

The HARDMath results are more mixed than PHYSICS, which is consistent with the benchmark’s stricter symbolic answer format and the need for exact final expressions. Even after regrading for mathematical equivalence and partial credit, prompt remains strongest on several categories, while memory banks help most on ODE and tie the prompt baseline on one of the integral splits.

Table 10: **Big Five contrastive generation judged by an LLM judge on Meta-Llama-3.1-8B-Instruct.** Columns report target-trait score, target-score shift from the plain model, non-target drift, contrastive margin, and generation-adjusted score, where  $\text{GAS} = \Delta_{\text{target}} - D_{\text{non-target}}$ . Contrastive margin is a separate auxiliary diagnostic.

Trait	Method	Score	Shift	Drift	Margin	GAS
Openness	Plain	4.54	+0.00	1.11	3.33	-1.110
	Prompt	4.79	+0.25	1.04	3.62	<b>-0.790</b>
	CAA	4.62	+0.08	1.10	3.29	-1.020
	Ours	4.50	-0.04	1.07	3.12	-1.110
Conscientiousness	Plain	4.83	+0.00	0.68	3.71	-0.680
	Prompt	4.79	-0.04	0.64	3.62	-0.680
	CAA	4.92	+0.09	0.66	3.88	-0.570
	Ours	4.96	+0.13	0.69	3.92	<b>-0.560</b>
Extraversion	Plain	3.50	+0.00	1.18	1.38	-1.180
	Prompt	4.33	+0.83	1.25	2.71	<b>-0.420</b>
	CAA	3.92	+0.42	1.18	1.83	-0.760
	Ours	4.12	+0.62	1.19	2.29	-0.570
Agreeableness	Plain	4.83	+0.00	0.96	3.79	-0.960
	Prompt	4.92	+0.09	0.55	3.83	<b>-0.460</b>
	CAA	4.88	+0.05	1.02	3.83	-0.970
	Ours	4.92	+0.09	0.95	3.88	-0.860
Neuroticism	Plain	3.62	+0.00	0.99	1.12	-0.990
	Prompt	4.29	+0.67	0.94	2.42	-0.270
	CAA	3.50	-0.12	0.93	1.00	-1.050
	Ours	4.42	+0.80	0.71	2.79	<b>0.090</b>
Average	Plain	4.26	+0.00	0.98	2.67	-0.984
	Prompt	4.62	+0.36	0.88	3.24	<b>-0.524</b>
	CAA	4.37	+0.11	0.98	2.77	-0.874
	Ours	4.58	+0.32	0.92	3.20	-0.602

### F.7 GSM8K and MMLU capability checks

These rows do not suggest catastrophic capability loss. The memory-bank condition stays close to the plain model and usually remains within the spread already induced by prompt or CAA steering.

### F.8 Mechanistic routing examples

Table 20 reports representative selector diagnostics from memory-bank runs. Each row freezes the selected layers and attention units chosen by the selector, then averages the diagnostic attention mass assigned to target, reference, and prompt banks over the selected units in the trace. The examples illustrate that the intervention is selective routing rather than uniform prompt prepending.

The warm and formal persistence examples show concentrated routing: roughly 91% of the measured bank/prompt attention mass goes to the target bank at the selected mid-to-late layers, corresponding to judged target/persistence/quality triples of 8.40/8.77/8.77 and 6.41/8.05/8.98. The dialogue-shift example uses an explicit opposite-style reference bank, producing a still-dominant target route but leaving nonzero prompt and reference mass that makes the update behavior auditable; its post-shift target and old-trait scores are 4.16 and 1.52, giving alignment 2.64.

### F.9 Outstanding ablations and omissions

We omit unfinished ablation sweeps rather than presenting unstable numbers. The main missing item is a fully frozen layer-count ablation that varies the number and identity of selected layers while keeping bank content fixed. That study would help isolate how much of MI’s gain comes from selective placement rather than from the bank text alone.

Table 11: **Big Five contrastive generation judged by an LLM judge on Qwen3-30B-A3B.** Columns report target-trait score, target-score shift from the plain model, non-target drift, contrastive margin, and generation-adjusted score, where  $GAS = \Delta_{\text{target}} - D_{\text{non-target}}$ . This is the detailed version of the matched-task summary in Table 1.

Trait	Method	Score	Shift	Drift	Margin	GAS
Openness	Plain	2.17	+0.00	0.83	0.67	-0.830
	Prompt	2.83	+0.66	0.83	1.67	-0.170
	CAA	1.83	-0.34	1.00	-0.33	-1.340
	Ours	3.83	+1.66	1.12	2.00	<b>0.540</b>
Conscientiousness	Plain	3.83	+0.00	0.71	2.83	-0.710
	Prompt	4.17	+0.34	0.58	3.17	-0.240
	CAA	3.83	+0.00	0.62	2.83	-0.620
	Ours	5.00	+1.17	0.92	4.00	<b>0.250</b>
Extraversion	Plain	2.00	+0.00	0.92	0.83	-0.920
	Prompt	3.67	+1.67	0.92	2.67	<b>0.750</b>
	CAA	2.00	+0.00	0.96	0.83	-0.960
	Ours	3.33	+1.33	1.17	0.83	0.160
Agreeableness	Plain	3.50	+0.00	0.62	2.50	-0.620
	Prompt	4.17	+0.67	0.71	3.17	-0.040
	CAA	3.50	+0.00	0.75	2.33	-0.750
	Ours	5.00	+1.50	0.88	4.00	<b>0.620</b>
Neuroticism	Plain	1.00	+0.00	0.96	-4.00	-0.960
	Prompt	2.67	+1.67	0.67	-0.33	<b>1.000</b>
	CAA	1.00	+0.00	0.96	-4.00	-0.960
	Ours	2.67	+1.67	1.04	-0.67	0.630
Average	Plain	2.50	+0.00	0.81	0.57	-0.808
	Prompt	3.50	+1.00	0.74	2.07	0.260
	CAA	2.43	-0.07	0.86	0.33	-0.926
	Ours	3.97	+1.47	1.02	2.03	<b>0.440</b>

Table 12: **Qwen3 long-context dialogue persistence by trait and prefill length.** Each method cell reports  $P/T/Q$ : conversation-level target persistence, mean turn-level target style score, and conversation-level overall quality. Prefill is non-task assistant-history context inserted before the dialogue. Prompt is the once-initialized visible-instruction baseline; Ours is memory-bank steering. Missing cells indicate no valid judged run after judge-completion filtering.

Trait	Prefill	Plain	Prompt	CAA	Ours
Warm	8k	9.04 / 8.68 / 9.19	9.19 / 8.95 / 9.34	8.94 / 8.41 / 9.02	8.51 / 8.29 / 8.39
	16k	9.01 / 8.62 / 9.14	9.12 / 8.79 / 9.21	8.91 / 8.43 / 9.00	8.90 / 8.43 / 8.92
	24k	8.96 / 8.64 / 9.10	9.06 / 8.73 / 9.13	8.94 / 8.48 / 8.99	8.91 / 8.47 / 9.00
Formal	8k	8.07 / 6.31 / 9.07	8.41 / 6.68 / 9.18	8.06 / 6.43 / 9.01	8.04 / 6.40 / 8.97
	16k	8.04 / 6.36 / 9.01	8.16 / 6.58 / 9.05	8.10 / 6.51 / 8.98	8.06 / 6.43 / 9.00
	24k	8.05 / 6.35 / 9.04	8.18 / 6.53 / 9.05	8.05 / 6.47 / 8.97	8.05 / 6.41 / 8.98
Assertive	8k	8.94 / 7.88 / 9.24	9.01 / 8.12 / 9.30	8.79 / 7.59 / 9.01	8.73 / 7.56 / 9.01
	16k	8.83 / 7.91 / 9.05	9.01 / 8.15 / 9.19	8.77 / 7.60 / 8.98	8.72 / 7.57 / 8.99
	24k	8.85 / 7.91 / 9.05	8.98 / 8.06 / 9.11	8.73 / 7.62 / 8.97	8.71 / 7.57 / 8.96
Cautious	8k	8.65 / 6.18 / 9.12	8.86 / 6.34 / 9.20	8.65 / 6.23 / 9.02	8.71 / 6.29 / 8.97
	16k	8.60 / 6.13 / 9.10	8.72 / 6.25 / 9.12	8.66 / 6.12 / 8.99	8.74 / 6.19 / 8.99
	24k	8.56 / 6.10 / 9.06	8.65 / 6.19 / 9.06	8.67 / 6.10 / 8.99	8.70 / 6.22 / 8.99
Dismissive	8k	1.00 / 1.01 / 9.69	1.61 / 1.26 / 9.49	1.00 / 1.04 / 9.28	2.35 / 1.99 / 6.56
	16k	1.00 / 1.02 / 9.54	1.05 / 1.05 / 9.60	1.01 / 1.03 / 9.17	1.85 / 1.84 / 6.51
	24k	1.00 / 1.01 / 9.58	1.00 / 1.02 / 9.58	1.00 / 1.04 / 9.23	1.68 / 1.60 / 6.55
Anxious	8k	4.96 / 1.67 / 8.90	5.59 / 2.14 / 8.90	5.73 / 1.96 / 8.55	6.23 / 2.54 / 6.53
	16k	4.99 / 1.74 / 8.73	4.94 / 1.73 / 8.81	5.86 / 2.01 / 8.52	6.21 / 2.39 / 7.12
	24k	4.69 / 1.75 / 8.75	4.88 / 1.74 / 8.77	6.05 / 2.03 / 8.51	6.27 / 2.27 / 7.35

Table 13: **Meta-Llama-3.1-8B-Instruct long-context dialogue persistence by trait and prefill length.** Each cell reports  $P/T/Q$ : conversation-level target persistence, mean turn-level target style score, and conversation-level overall quality. The main text reports only the model-level averages; this table gives the full trait×budget breakdown. Plain is the opposite-prefill baseline. Prompt adds one visible target-style system instruction before the same opposite-prefill context. CAA is the frozen post-attention residual baseline (layer 14, scale 2), and Ours reports the frozen memory-bank configuration used in the final judged audit.

Trait	Prefill	Plain	Prompt	CAA	Ours
Warm	8k	7.66 / 7.38 / 8.57	8.76 / 8.06 / 8.99	8.23 / 7.49 / 8.83	8.08 / 7.41 / 8.83
	16k	8.17 / 7.52 / 8.83	8.75 / 8.00 / 8.95	7.92 / 7.47 / 8.71	8.26 / 7.43 / 8.83
	24k	7.72 / 7.60 / 8.61	8.70 / 8.01 / 9.00	8.29 / 7.71 / 8.81	7.92 / 7.46 / 8.70
Formal	8k	7.66 / 6.09 / 8.79	8.01 / 6.20 / 8.98	8.04 / 6.56 / 9.00	7.69 / 6.01 / 8.76
	16k	7.51 / 6.05 / 8.75	7.96 / 6.27 / 8.93	8.11 / 6.58 / 9.00	7.51 / 6.01 / 8.63
	24k	7.48 / 6.04 / 8.67	7.93 / 6.26 / 8.93	8.06 / 6.62 / 8.99	7.52 / 5.99 / 8.64
Assertive	8k	7.80 / 6.79 / 8.78	7.91 / 7.10 / 8.82	8.32 / 7.25 / 8.98	7.54 / 6.37 / 8.51
	16k	6.55 / 6.26 / 7.87	7.68 / 6.95 / 8.58	8.12 / 7.22 / 8.89	6.95 / 6.25 / 8.00
	24k	7.10 / 6.50 / 8.19	7.67 / 6.89 / 8.61	7.99 / 7.21 / 8.87	7.04 / 6.21 / 7.97
Cautious	8k	7.36 / 5.73 / 8.46	8.39 / 6.39 / 9.00	7.84 / 6.17 / 8.77	7.46 / 5.71 / 8.48
	16k	7.47 / 5.70 / 8.62	8.32 / 6.37 / 8.97	7.92 / 6.16 / 8.86	7.34 / 5.70 / 8.34
	24k	7.47 / 5.85 / 8.57	8.22 / 6.30 / 8.97	7.98 / 6.28 / 8.80	7.87 / 5.86 / 8.78
Dismissive	8k	1.00 / 1.06 / 8.69	7.62 / 6.06 / 5.87	1.02 / 1.19 / 8.74	3.63 / 2.74 / 4.45
	16k	1.01 / 1.06 / 8.71	8.41 / 7.09 / 5.39	1.10 / 1.20 / 8.66	4.08 / 2.69 / 4.14
	24k	1.03 / 1.07 / 8.73	8.45 / 6.87 / 5.37	1.21 / 1.16 / 8.57	3.92 / 2.62 / 4.46
Anxious	8k	5.88 / 2.09 / 8.06	6.11 / 2.20 / 8.04	6.08 / 2.29 / 8.03	6.53 / 2.72 / 7.78
	16k	6.09 / 2.14 / 8.07	6.56 / 2.88 / 8.07	6.13 / 2.29 / 8.07	6.49 / 2.67 / 7.78
	24k	6.12 / 2.14 / 8.03	6.46 / 2.47 / 8.13	6.16 / 2.29 / 8.04	6.50 / 2.66 / 7.89

Table 14: **Qwen3 dialogue-shift post-shift alignment by transition and dialogue length.** Entries report Align on post-shift turns. Bold marks the best matched-budget method in each row among Plain, Prompt-init, CAA, and Ours. Prompt-repl. is shown only as an audit because it adds visible steering text at the shift point.

Transition	Turns	Metric	Plain	Prompt-init	CAA	Ours	Prompt-repl.
Warm→Assertive	8	Align	-0.04	-0.46	<b>0.19</b>	-0.50	-0.29
Warm→Assertive	16	Align	-0.23	-0.25	<b>0.00</b>	-0.34	-0.29
Warm→Assertive	24	Align	-0.40	-0.43	<b>-0.30</b>	-0.80	-0.35
Assertive→Warm	8	Align	1.33	1.17	1.56	<b>1.88</b>	1.12
Assertive→Warm	16	Align	1.43	1.38	1.66	<b>2.29</b>	1.34
Assertive→Warm	24	Align	1.25	1.24	1.38	<b>1.90</b>	1.17
Formal→Cautious	8	Align	0.22	-0.06	<b>0.46</b>	0.06	0.11
Formal→Cautious	16	Align	-0.14	-0.21	<b>0.19</b>	-0.02	-0.12
Formal→Cautious	24	Align	-0.29	-0.44	-0.17	<b>-0.15</b>	-0.06
Cautious→Formal	8	Align	1.50	1.58	<b>1.69</b>	1.42	1.67
Cautious→Formal	16	Align	0.79	0.89	<b>1.16</b>	0.71	1.21
Cautious→Formal	24	Align	0.82	1.05	<b>1.29</b>	0.93	1.09
Dismissive→Anxious	8	Align	0.83	1.00	1.96	<b>2.83</b>	2.06
Dismissive→Anxious	16	Align	1.02	1.55	1.65	<b>2.74</b>	4.17
Dismissive→Anxious	24	Align	1.11	1.02	<b>2.52</b>	2.48	2.86
Anxious→Dismissive	8	Align	-1.17	-0.67	<b>0.12</b>	-1.17	0.00
Anxious→Dismissive	16	Align	-0.93	-0.79	-0.44	<b>-0.36</b>	0.21
Anxious→Dismissive	24	Align	-0.77	-0.55	-0.42	<b>-0.32</b>	-0.86

Table 15: **Qwen3 dialogue-shift post-shift turn quality by transition and dialogue length.** Entries report  $Q_{\text{turn}}$  on post-shift turns. Bold marks the best matched-budget method in each row among Plain, Prompt-init, CAA, and Ours. Prompt-repl. is shown only as an audit because it adds visible steering text at the shift point.

Transition	Turns	Metric	Plain	Prompt-init	CAA	Ours	Prompt-repl.
Warm→Assertive	8	$Q_{\text{turn}}$	8.67	<b>8.72</b>	8.64	7.86	8.65
Warm→Assertive	16	$Q_{\text{turn}}$	8.73	<b>8.77</b>	8.71	7.64	8.78
Warm→Assertive	24	$Q_{\text{turn}}$	<b>8.70</b>	8.66	8.59	7.25	8.63
Assertive→Warm	8	$Q_{\text{turn}}$	8.47	<b>8.62</b>	8.41	7.27	8.58
Assertive→Warm	16	$Q_{\text{turn}}$	<b>8.58</b>	8.55	8.45	6.45	8.51
Assertive→Warm	24	$Q_{\text{turn}}$	<b>8.55</b>	8.53	8.47	6.44	8.57
Formal→Cautious	8	$Q_{\text{turn}}$	<b>8.60</b>	8.58	8.51	8.44	8.49
Formal→Cautious	16	$Q_{\text{turn}}$	<b>8.55</b>	8.50	8.54	8.27	8.49
Formal→Cautious	24	$Q_{\text{turn}}$	8.39	<b>8.43</b>	8.35	8.19	8.40
Cautious→Formal	8	$Q_{\text{turn}}$	8.46	8.46	<b>8.50</b>	7.67	8.42
Cautious→Formal	16	$Q_{\text{turn}}$	8.58	<b>8.63</b>	8.59	7.47	8.59
Cautious→Formal	24	$Q_{\text{turn}}$	8.66	<b>8.70</b>	8.68	7.89	8.61
Dismissive→Anxious	8	$Q_{\text{turn}}$	<b>8.56</b>	8.49	8.33	6.28	7.53
Dismissive→Anxious	16	$Q_{\text{turn}}$	<b>8.56</b>	8.24	8.31	4.79	6.27
Dismissive→Anxious	24	$Q_{\text{turn}}$	8.44	<b>8.52</b>	7.42	3.98	6.99
Anxious→Dismissive	8	$Q_{\text{turn}}$	<b>8.62</b>	8.29	8.03	7.33	7.50
Anxious→Dismissive	16	$Q_{\text{turn}}$	<b>8.18</b>	7.95	7.72	5.27	6.64
Anxious→Dismissive	24	$Q_{\text{turn}}$	<b>8.15</b>	8.12	8.05	4.16	7.70

Table 16: **Meta-Llama-3.1-8B-Instruct halfway-shift dialogue summary.** Each breakdown is split into two metric rows: post-shift alignment Align and judged turn quality  $Q_{\text{turn}}$ . Bold marks the best method in each metric row. CAA is the frozen layer-14, scale-2 post-attention residual baseline; Ours is memory-bank summary update.

Breakdown	Metric	Plain	Prompt-init	CAA	Ours
Overall	Align	1.112	1.178	<b>1.554</b>	1.516
	$Q_{\text{turn}}$	<b>7.72</b>	7.58	7.34	7.00
Anxious→Dismissive	Align	1.654	2.212	<b>2.808</b>	2.692
	$Q_{\text{turn}}$	<b>5.92</b>	5.49	4.63	4.49
Assertive→Warm	Align	1.026	1.087	<b>1.209</b>	1.148
	$Q_{\text{turn}}$	8.30	<b>8.35</b>	8.23	8.03
Cautious→Formal	Align	0.835	0.852	<b>1.157</b>	0.913
	$Q_{\text{turn}}$	8.33	<b>8.35</b>	8.27	7.87
Dismissive→Anxious	Align	3.615	3.240	4.298	<b>4.577</b>
	$Q_{\text{turn}}$	<b>7.06</b>	6.44	5.98	5.85
Formal→Cautious	Align	-0.252	<b>-0.113</b>	-0.191	-0.209
	$Q_{\text{turn}}$	8.11	<b>8.14</b>	8.05	7.77
Warm→Assertive	Align	0.087	0.087	<b>0.426</b>	0.383
	$Q_{\text{turn}}$	8.40	8.40	<b>8.48</b>	7.65
8 turns	Align	1.185	1.204	<b>1.398</b>	1.278
	$Q_{\text{turn}}$	<b>7.84</b>	7.57	7.52	7.22
16 turns	Align	1.373	1.429	<b>1.833</b>	1.829
	$Q_{\text{turn}}$	<b>7.56</b>	7.36	7.15	6.88
24 turns	Align	0.873	0.964	<b>1.380</b>	1.344
	$Q_{\text{turn}}$	<b>7.82</b>	7.76	7.43	7.03

Table 17: **Full PHYSICS subject×mode matrix on Qwen3-30B-A3B**. Values are mean 0–5 partial-credit judge scores, normalized to percent and averaged over three grading passes. Chain of thought (CoT) denotes Qwen3 thinking mode; no-CoT disables it.

Domain	Mode	Plain (%) ↑	Prompt (%) ↑	Ours (%) ↑
Classical mechanics	no-CoT	66.0	<b>69.4</b>	68.2
Classical mechanics	CoT	82.0	84.0	<b>85.4</b>
Quantum mechanics	no-CoT	65.4	63.5	<b>68.1</b>
Quantum mechanics	CoT	69.2	75.0	<b>76.6</b>
Atomic physics	no-CoT	71.4	71.8	<b>73.2</b>
Atomic physics	CoT	80.2	79.5	<b>84.2</b>
Optics	no-CoT	69.2	72.9	<b>74.2</b>
Optics	CoT	<b>85.0</b>	83.2	83.0
Electromagnetism	no-CoT	60.6	63.6	<b>64.4</b>
Electromagnetism	CoT	75.8	76.6	<b>77.8</b>
Thermodynamics/statistical mechanics	no-CoT	72.2	76.4	<b>76.8</b>
Thermodynamics/statistical mechanics	CoT	89.4	89.0	<b>90.6</b>

Table 18: **Full HARDMath category breakdown on Qwen3-30B-A3B with chain of thought**. Values are category partial-credit total / maximum partial-credit total, with the normalized percentage in parentheses.

Category	Plain	Prompt	Ours
Integral 0	13.5 / 30 (45.0)	<b>14.5 / 30 (48.3)</b>	<b>14.5 / 30 (48.3)</b>
Integral 1	<b>13.5 / 30 (45.0)</b>	13.0 / 30 (43.3)	<b>13.5 / 30 (45.0)</b>
Laplace-integral 0	26.0 / 30 (86.7)	<b>29.0 / 30 (96.7)</b>	28.0 / 30 (93.3)
Laplace-integral 1	25.0 / 30 (83.3)	<b>29.0 / 30 (96.7)</b>	22.0 / 30 (73.3)
ODE	7.0 / 54 (13.0)	11.0 / 54 (20.4)	<b>14.0 / 54 (25.9)</b>
Polynomial roots	12.0 / 63 (19.0)	<b>22.0 / 63 (34.9)</b>	15.0 / 63 (23.8)
Nondim-symbolic	<b>65.0 / 65 (100.0)</b>	<b>65.0 / 65 (100.0)</b>	<b>65.0 / 65 (100.0)</b>
Nondim-numeric	59.0 / 60 (98.3)	<b>60.0 / 60 (100.0)</b>	59.0 / 60 (98.3)
Overall	220.0 / 362 (60.8)	<b>243.5 / 362 (67.3)</b>	231.0 / 362 (63.8)

Table 19: **Qwen3 GSM8K and MMLU capability checks**. These appendix results are intended as coarse capability-preservation checks rather than main steering results.

Benchmark	Model	Trait/Bank	Plain	Prompt	CAA	Ours
GSM8K	Qwen3-30B-A3B	Warm	0.975	0.960	0.970	0.960
GSM8K	Qwen3-30B-A3B	Formal	0.970	0.960	0.970	0.955
GSM8K	Qwen3-30B-A3B	Direct	0.970	0.950	0.975	0.950
GSM8K	Qwen3-30B-A3B	Careful	0.970	0.945	0.955	0.945
GSM8K	Qwen3-30B-A3B	Curt	0.970	0.910	0.955	0.955
GSM8K	Qwen3-30B-A3B	Anxious	0.970	0.935	0.965	0.940
MMLU	Qwen3-30B-A3B	Warm	0.768	0.772	0.772	0.772
MMLU	Qwen3-30B-A3B	Formal	0.768	0.718	0.768	0.768
MMLU	Qwen3-30B-A3B	Direct	0.768	0.784	0.768	0.764
MMLU	Qwen3-30B-A3B	Careful	0.768	0.756	0.768	0.768
MMLU	Qwen3-30B-A3B	Curt	0.768	0.776	0.768	0.764
MMLU	Qwen3-30B-A3B	Anxious	0.768	0.706	0.768	0.764

Table 20: **Representative mechanistic routing examples.** Bank masses are averaged over selected attention units in selector diagnostic traces. Target/ref slots are latent KV slots. Selected units are heads for standard attention, or grouped-query KV units expanded to the corresponding query heads.

Example	Selected layers	Slots (target/ref)	Units	Target mass	Ref. mass	Prompt mass
Warm persistence	12, 14, 16, 18, 20, 22	498 / 0	24	0.911	0.000	0.089
Formal persistence	12, 14, 16, 18, 20, 22	474 / 0	24	0.911	0.000	0.089
Dismissive→Anxious	16, 18, 20, 24, 26, 32	480 / 432	20	0.685	0.126	0.190

## G Technical derivations

### G.1 Bank-mixture derivation

Let  $\mathcal{I}_b$  index the slots belonging to bank  $b$ . Concatenated attention with bank-specific slot bias gives

$$\tilde{\alpha}_{t,m}^{(b)} = \frac{\exp(s_{t,m}^{(b)} + c_t^{(b)})}{\sum_{b'} \sum_{r \in \mathcal{I}_{b'}} \exp(s_{t,r}^{(b')} + c_t^{(b')})}.$$

Factor the numerator as

$$\exp(s_{t,m}^{(b)} + c_t^{(b)}) = \left( \sum_{r \in \mathcal{I}_b} \exp(s_{t,r}^{(b)}) \right) \frac{\exp(s_{t,m}^{(b)})}{\sum_{r \in \mathcal{I}_b} \exp(s_{t,r}^{(b)})} \exp(c_t^{(b)}).$$

Define the within-bank softmax

$$\alpha_{t,m}^{(b)} = \frac{\exp(s_{t,m}^{(b)})}{\sum_{r \in \mathcal{I}_b} \exp(s_{t,r}^{(b)})}$$

and bank evidence

$$\tilde{\beta}_t^{(b)} = \log \sum_{r \in \mathcal{I}_b} \exp(s_{t,r}^{(b)}) + c_t^{(b)}.$$

Then  $\tilde{\alpha}_{t,m}^{(b)} = \pi_t^{(b)} \alpha_{t,m}^{(b)}$ , where

$$\pi_t^{(b)} = \frac{\exp(\tilde{\beta}_t^{(b)})}{\sum_{b'} \exp(\tilde{\beta}_t^{(b')})}.$$

Therefore

$$o_t^* = \sum_b \sum_{m \in \mathcal{I}_b} \tilde{\alpha}_{t,m}^{(b)} v_m^{(b)} = \sum_b \pi_t^{(b)} \sum_{m \in \mathcal{I}_b} \alpha_{t,m}^{(b)} v_m^{(b)} = \sum_b \pi_t^{(b)} o_t^{(b)}.$$

Subtracting  $\log M_b$  from each bank evidence gives the size-normalized version in Eq. (5).

### G.2 RoPE derivation

With RoPE, a prompt score between query position  $t$  and key position  $j$  is

$$\frac{\langle R_t \bar{q}_t, R_j \bar{k}_j \rangle}{\sqrt{d_h}} = \frac{\langle \bar{q}_t, R_{j-t} \bar{k}_j \rangle}{\sqrt{d_h}}.$$

For a canonical key  $\tilde{k}_m$ , assigning virtual relative phase  $\delta_m$  gives

$$\frac{\langle R_t^{-1} q_t, R_{\delta_m} \tilde{k}_m \rangle}{\sqrt{d_h}} = \frac{\langle \bar{q}_t, R_{\delta_m} \tilde{k}_m \rangle}{\sqrt{d_h}}.$$

The memory score therefore depends on the chosen relative phase, not on the absolute position at which the bank was built. The default  $\delta_m = 0$  gives a position-agnostic reminder slot.